TCAD simulations of signal sharing in DC-RSD LGAD devices for future 4D tracking

A. Fondacci[3,1], **T. Croci**[1], A. Morozzi[1], F. Moscatelli[2,1], D. Passeri[3,1], L. Menzio[5,4], M. Ferrero[4], V. Sola[5,4], R. Arcidiacono[6,4] and N. Cartiglia[4]

(1) Istituto Nazionale di Fisica Nucleare (INFN), Perugia, Italy
(2) Istituto Officina dei Materiali (IOM) CNR, Perugia, Italy
(3) Dipartimento di Ingegneria, Università di Perugia, Perugia, Italy
(4) Istituto Nazionale di Fisica Nucleare (INFN), Torino, Italy
(5) Dipartimento di Fisica, Università di Torino, Torino, Italy
(6) Dipartimento di Scienze del Farmaco, UPO, Novara, Italy

TREDI 2024, Torino - February 22, 2023

High-Energy Physics (HEP) experiments at future colliders

Requirements for the trackers:

- **Spatial** resolution $\sim 5\ \mu m$
- **Temporal** resolution $\sim 10\ ps$
- Very low **material budget**
  Sensor + elect. $< 100\ \mu m$ *of silicon*
- Very low **power consumption**
  Air cooling $< 0.2\ W/cm^2$

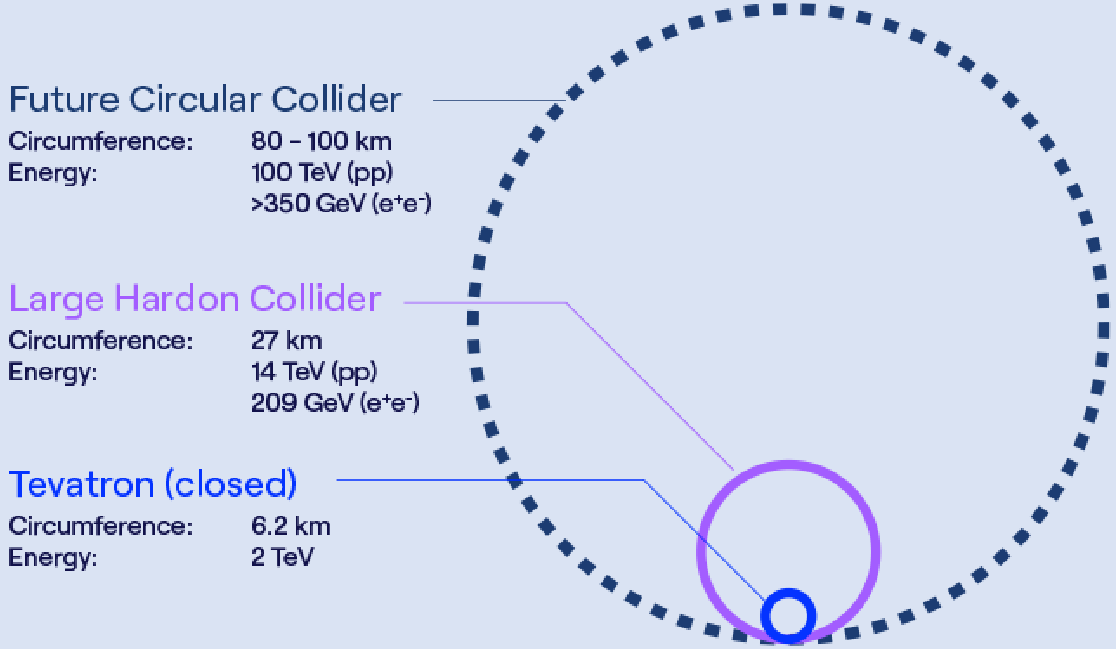

4D trackers should be the basic option for future detection systems!

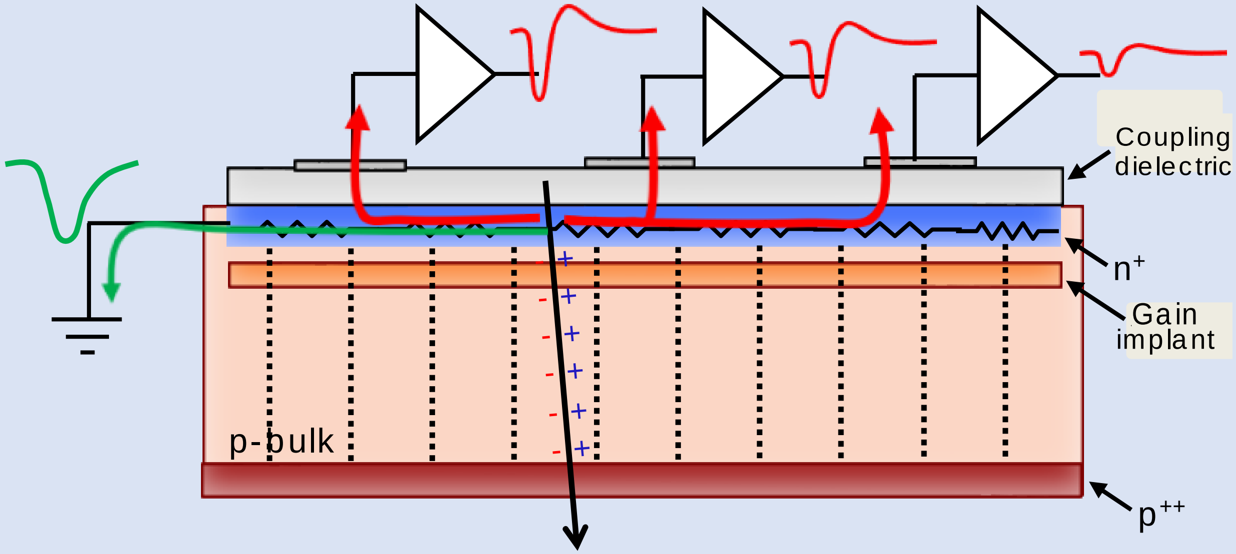

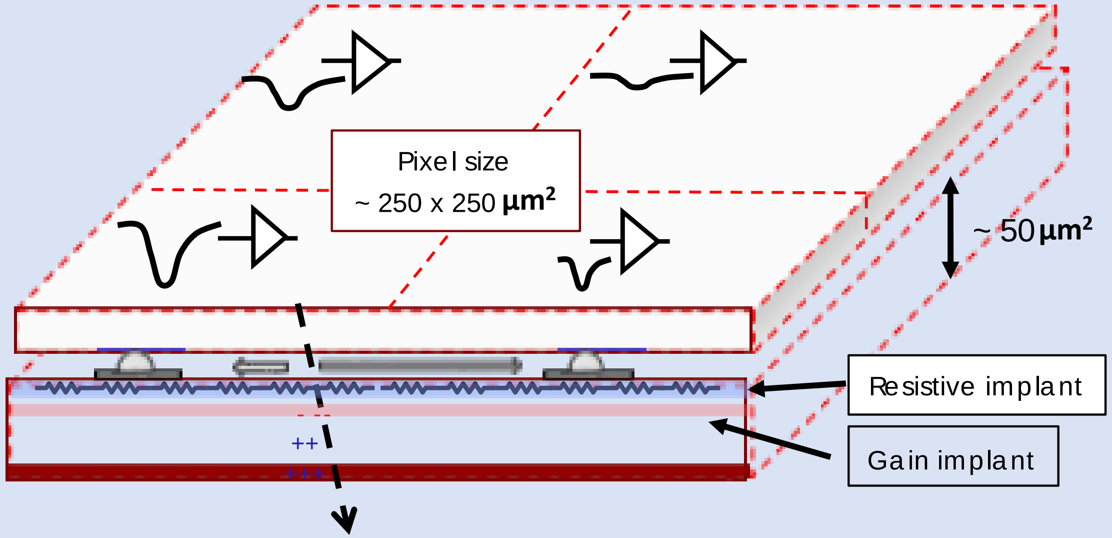

Resistive Silicon Detector (RSD)

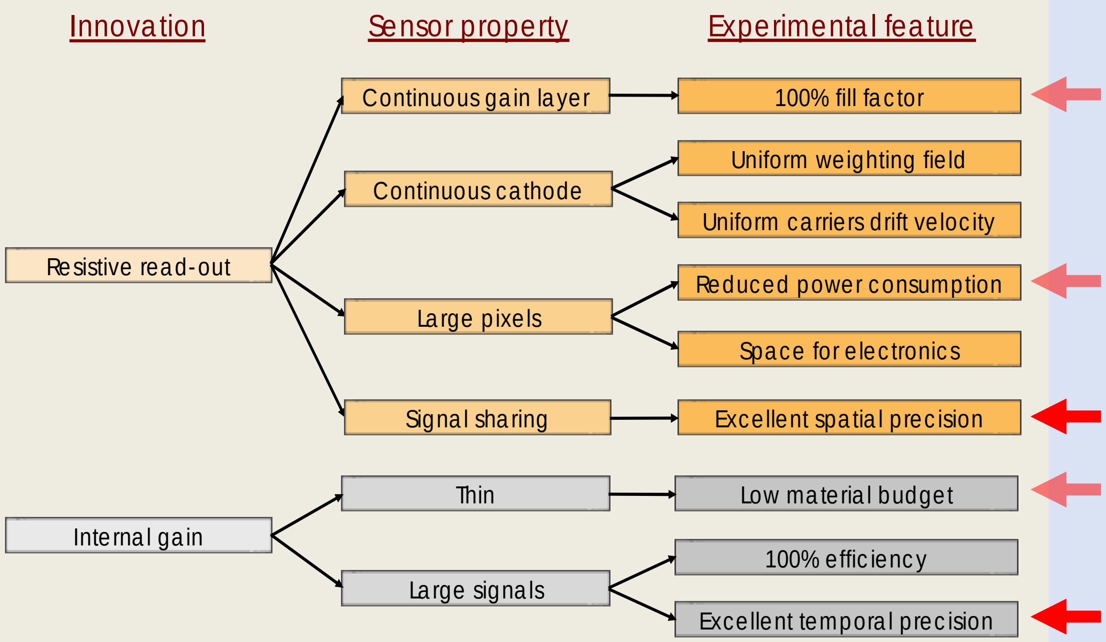

Emerging technology** for **4D tracking

[1] R. Arcidiacono et al., Nucl. Inst. and Meth. in Phys. Res. A, 1057 (2023) 168671.

Resistive Silicon Detectors (RSDs)

AC-RSD LGAD

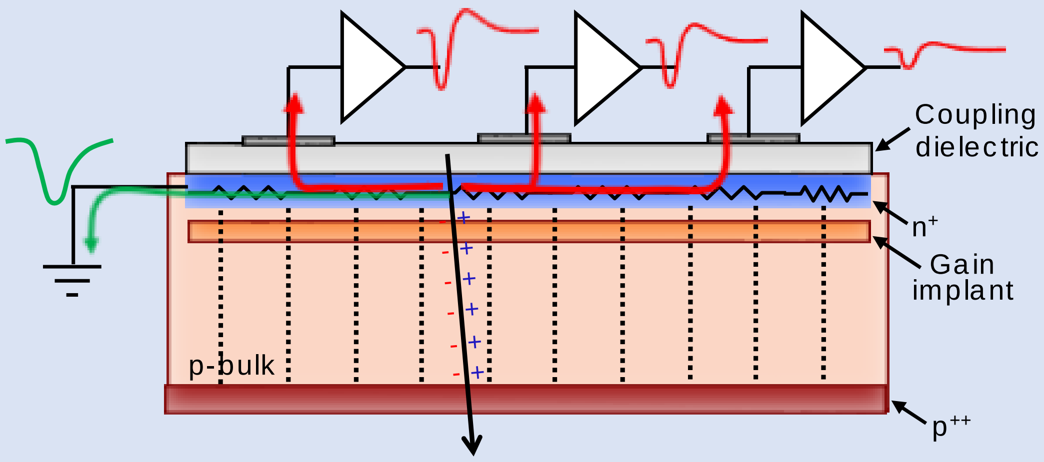

1. Long-tail bipolar signals
2. Position-dependent spatial resolution
3. Baseline fluctuation
4. Not easily scalable to large-area sensors

Resistive Silicon Detectors (RSDs)

AC-RSD LGAD

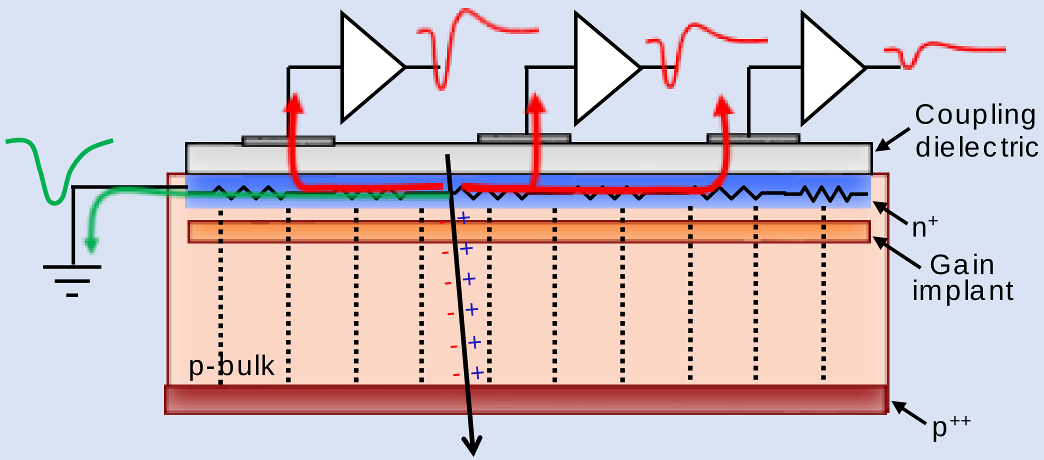

1. Long-tail bipolar signals
2. Position-dependent spatial resolution
3. Baseline fluctuation
4. Not easily scalable to large-area sensors

DC-RSD LGAD

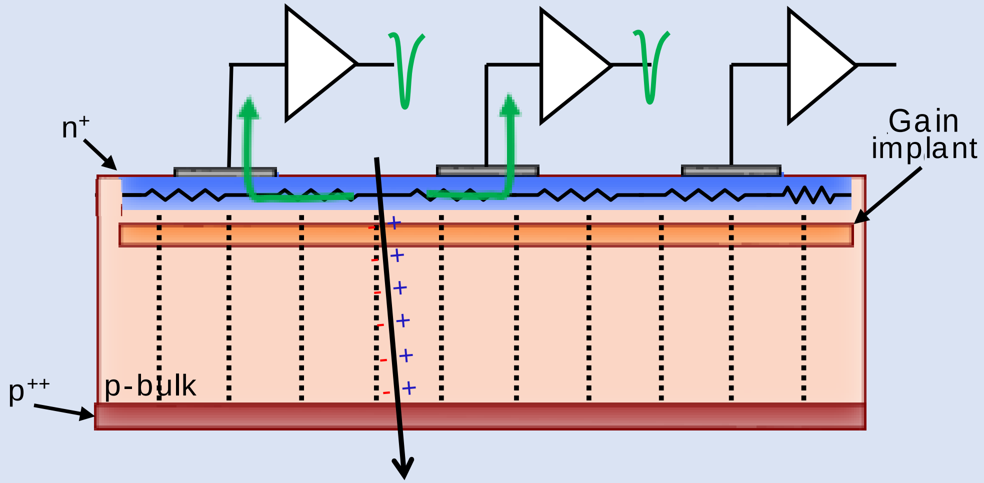

1. Unipolar signals
2. Well-confined charge sharing
3. Absence of baseline fluctuation
4. Large sensitive areas ($\sim cm$)

Simulation of DC-RSD: mixed-mode approach

Step 1: Spice (circuit-level) simulations

Accounting for an equivalent lumped-element electrical model (Fig. 1) in Spice environment, simulation of the output waveforms (Fig. 2-3) by injecting a test input signal

→ identification of the values of the key design parameters and reconstruction of the particle impact positions (Fig. 4) with very short simulation times [8].

Fig. 1

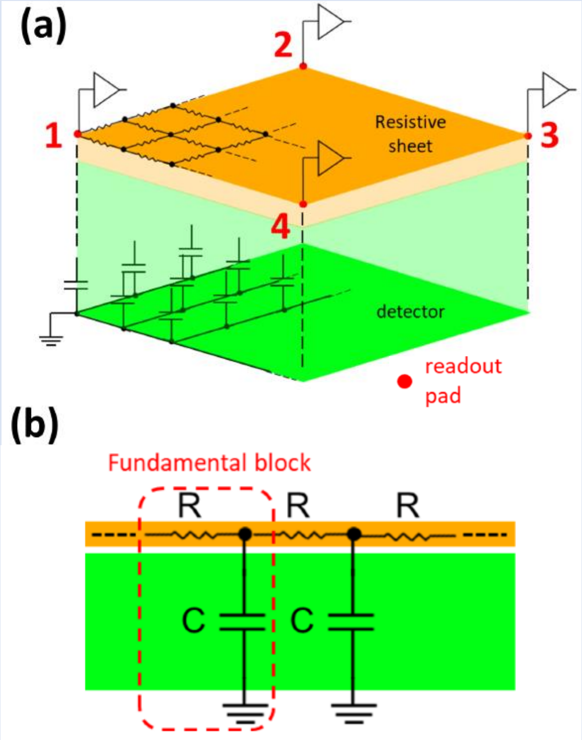

Fig. 2

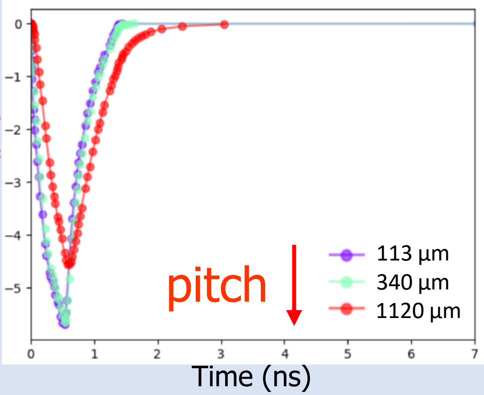

Fig. 3

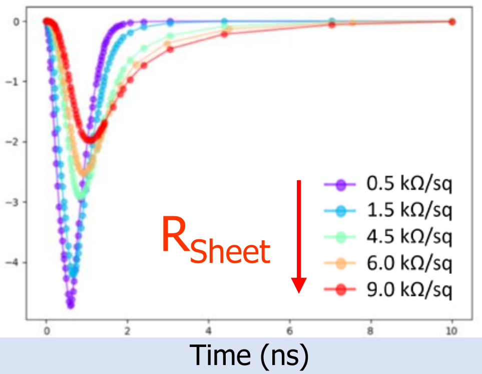

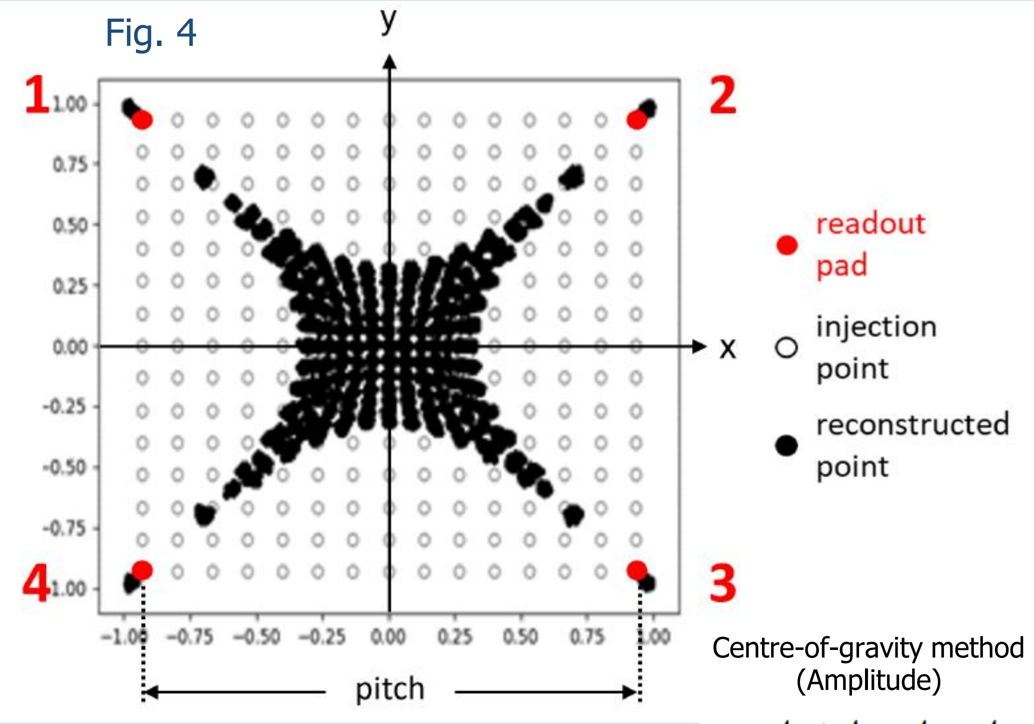

Centre-of-gravity method (Amplitude)

$$x = \frac{A_2 + A_3 - A_1 - A_4}{A_{tot}}$$

$$y = \frac{A_2 + A_1 - A_4 - A_3}{A_{tot}}$$

[2] L. Menzio et al., Nucl. Inst. and Meth. in Phys. Res. A, 1041 (2022) 167374.

Simulation of DC-RSD: mixed-mode approach

Step 2: TCAD (device-level) simulation

Full 3D TCAD simulation to characterize the device behavior in terms of response after the passage of a minimum ionizing particle (MIP) (Fig. 7)

→ the key features of the RSD' design, i.e. excellent timing and spatial resolutions (few tens of ps and μm), are maintained with the new paradigm of DC-RSDs.

Fig. 5

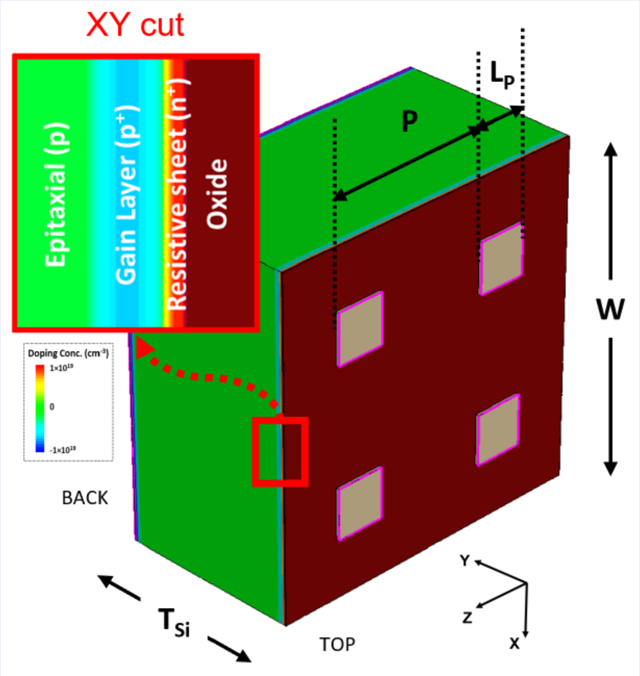

[3] T. Croci *et al.*, IEEE Trans. Nucl. Sci. doi: 10.1109/TNS.2024.3356826.

Fig. 6

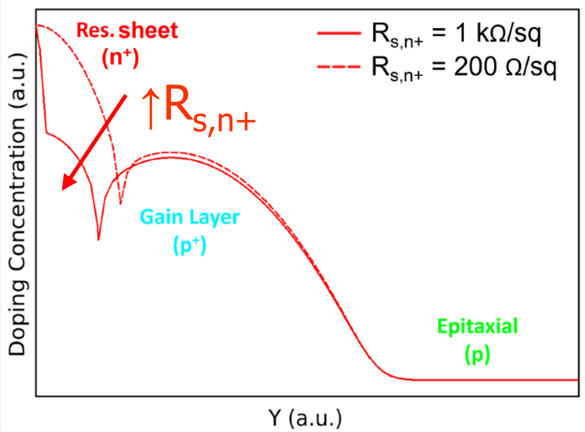

Fig. 7

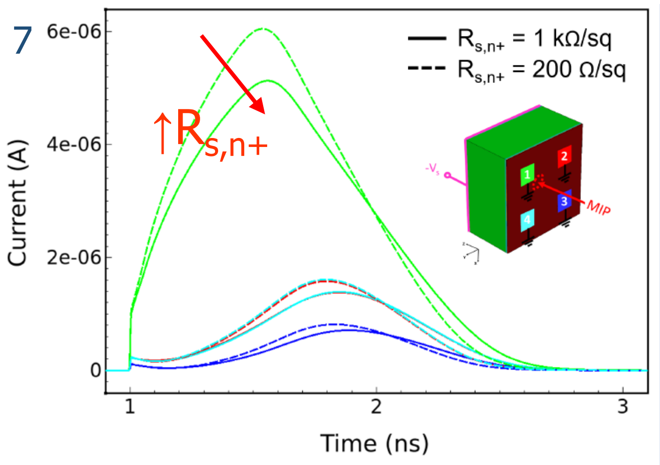

Fig. 8

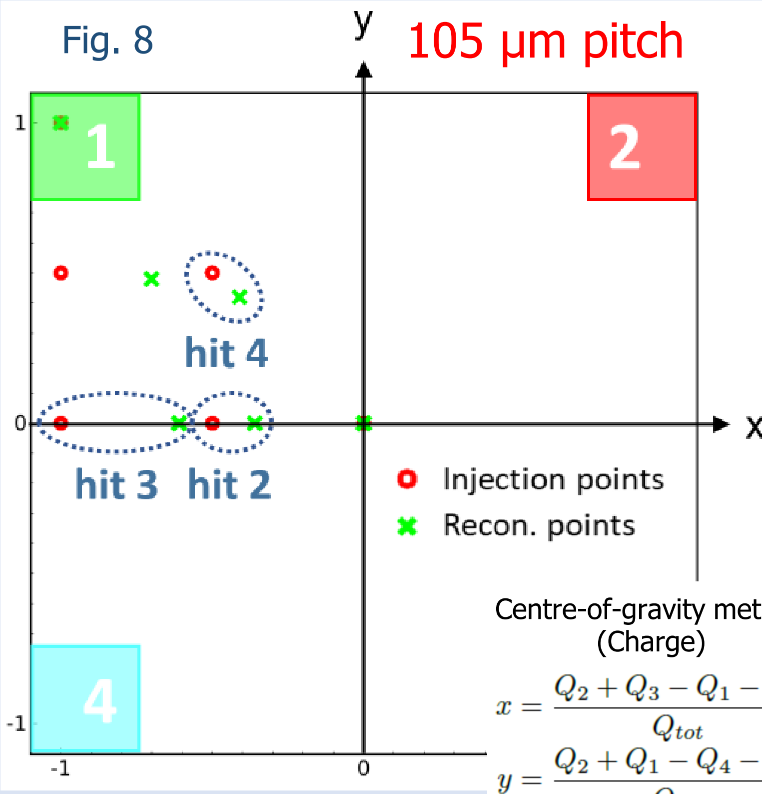

Centre-of-gravity method (Charge)

$$x = \frac{Q_2 + Q_3 - Q_1 - Q_4}{Q_{tot}}$$

$$y = \frac{Q_2 + Q_1 - Q_4 - Q_3}{Q_{tot}},$$

Improving signal confinement in DC-RSD

(Total) **current density map** → **signal distribution** in the n^+-resistive plane

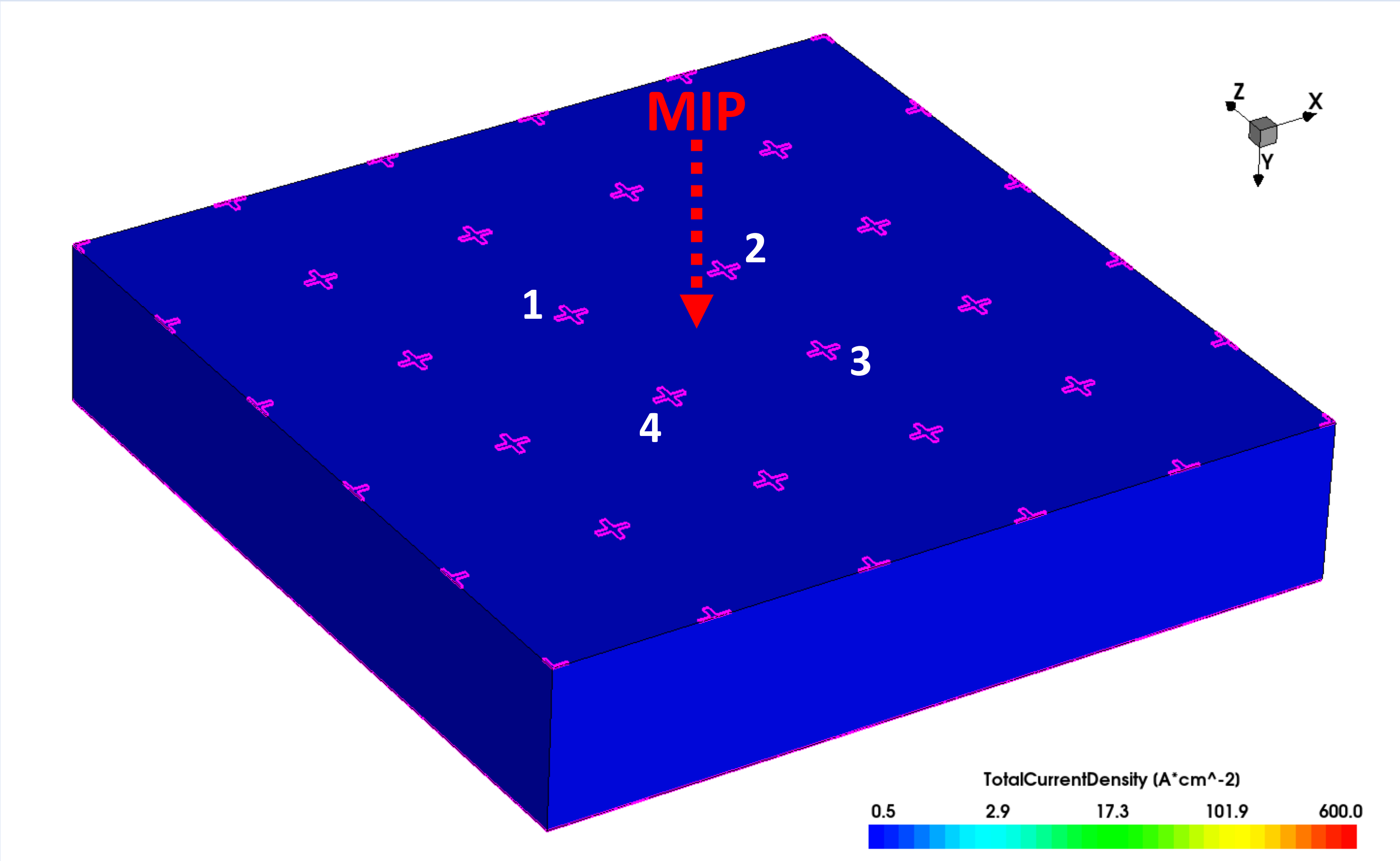

Minimum Ionizing Particle (MIP)

<u>Simulation setup</u>:

- 3D **PIN** diode ($R_S = 2\ k\Omega/sq$);
- 5×5-pixel matrix;
- Pitch: **20 µm**
- Stimulus: 1 MIP;
- Temperature: 300 K;
- Avalanche Model: Massey;
- Substrate voltage: -200 V.

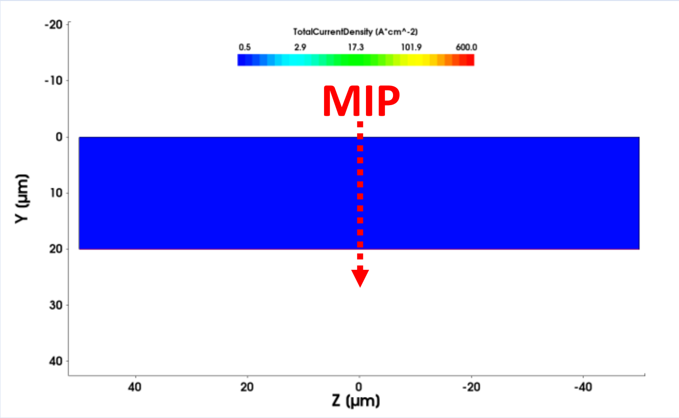

Playing with pad shape and dimension

Improving signal confinement: cross-shaped pad

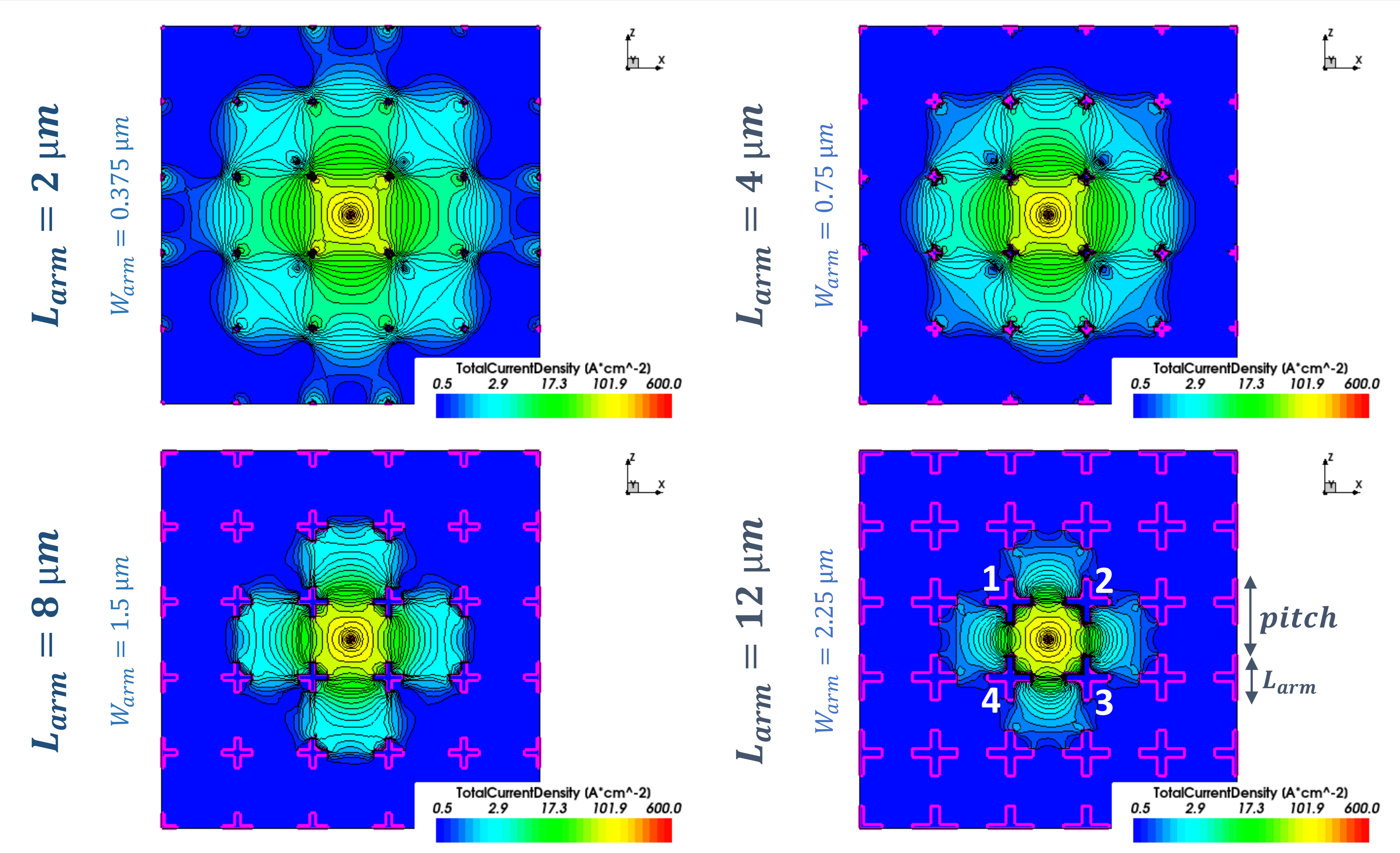

Playing with pad shape and dimension

Improving signal confinement: bar-shaped pad

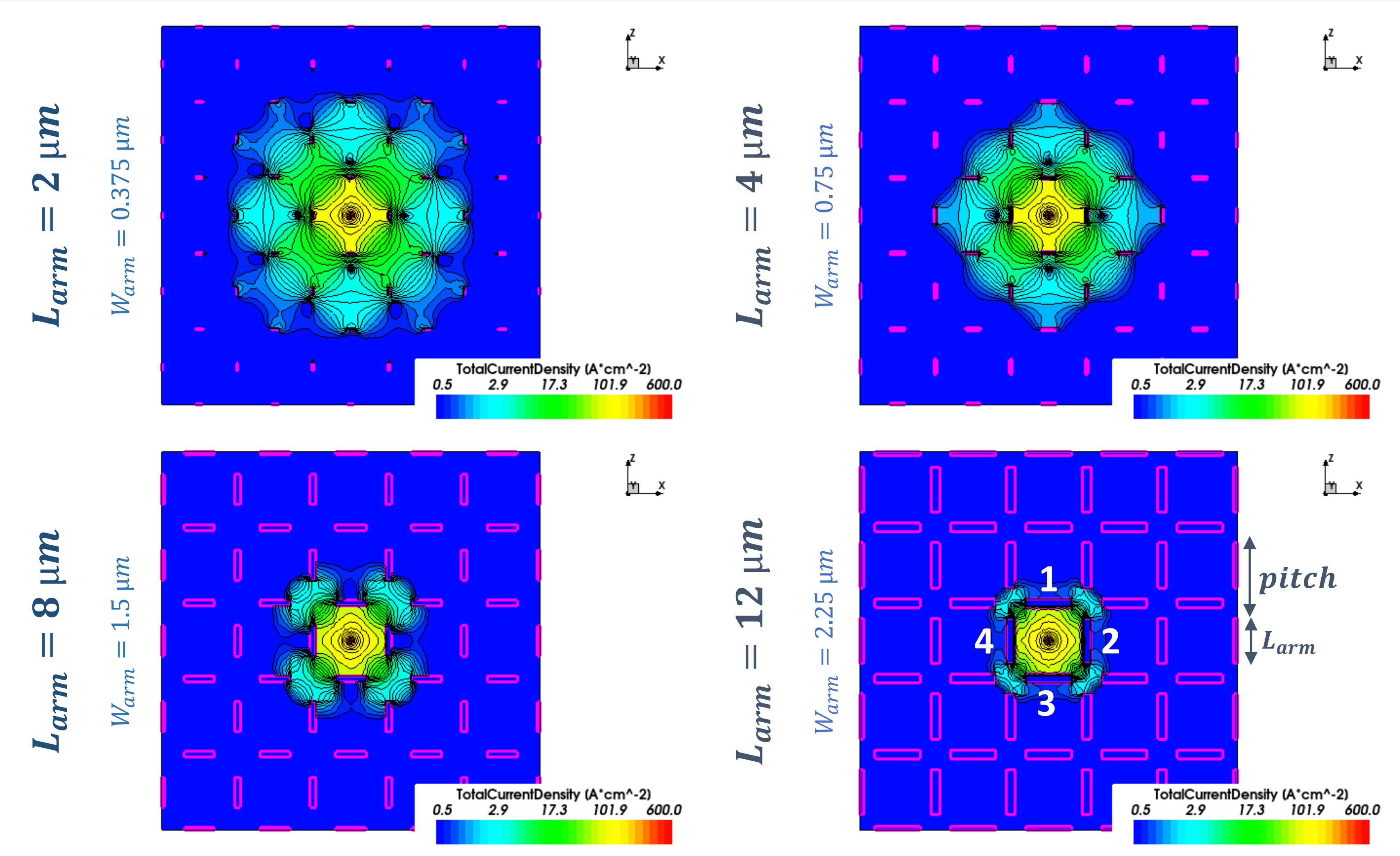

Playing with pad shape and dimension

Hit reconstruction vs. pad dimension

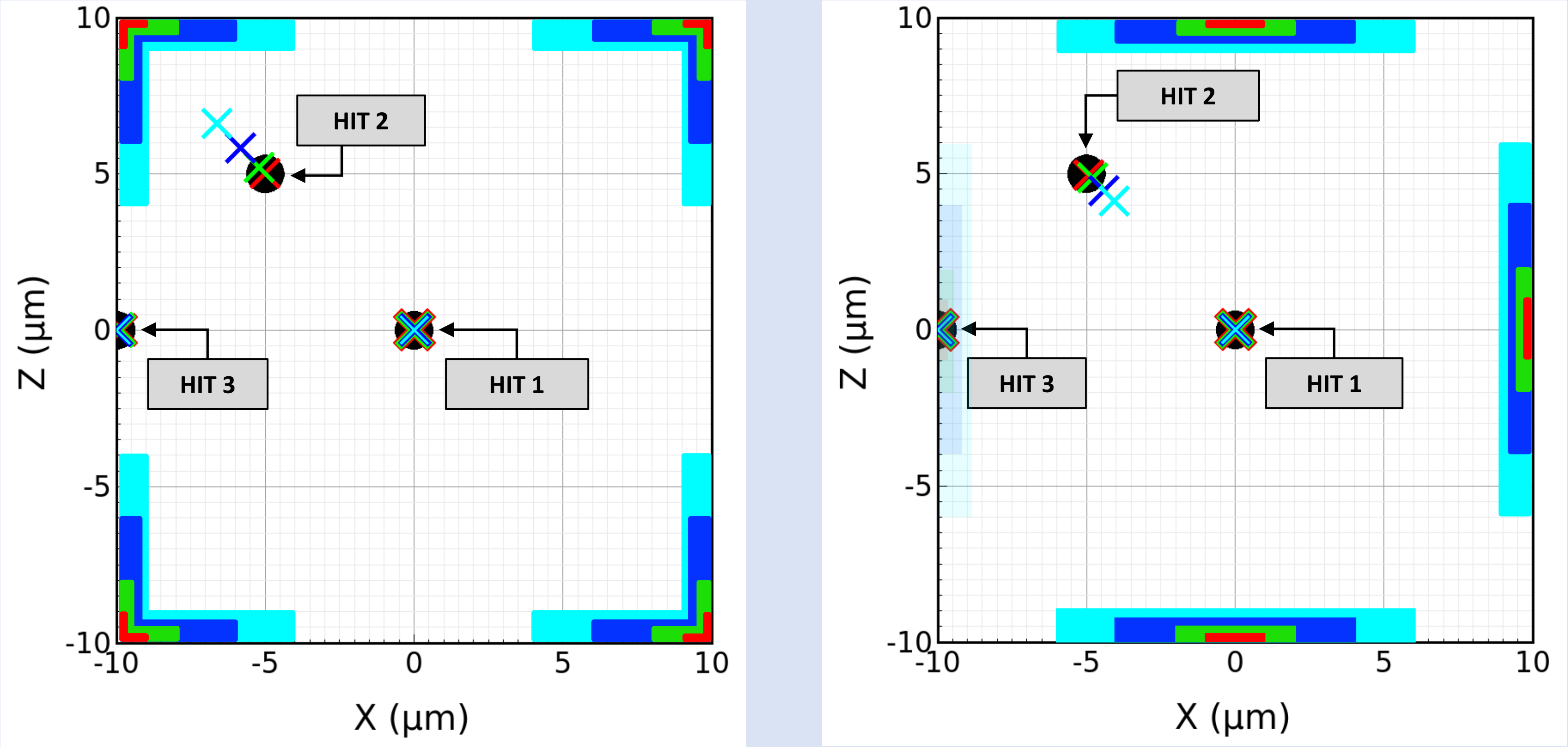

If the particle hits a pad or very close to it,
all the charge is picked up by that pad

*Make the **electrodes small** so as not to distort the reconstruction of the hit position*

Playing with pad shape and dimension

Improving signal confinement: cross vs. bar-shaped pad

36 electrodes

*The four pads (1, 2, 3 and 4) collect **96%** of the charge*

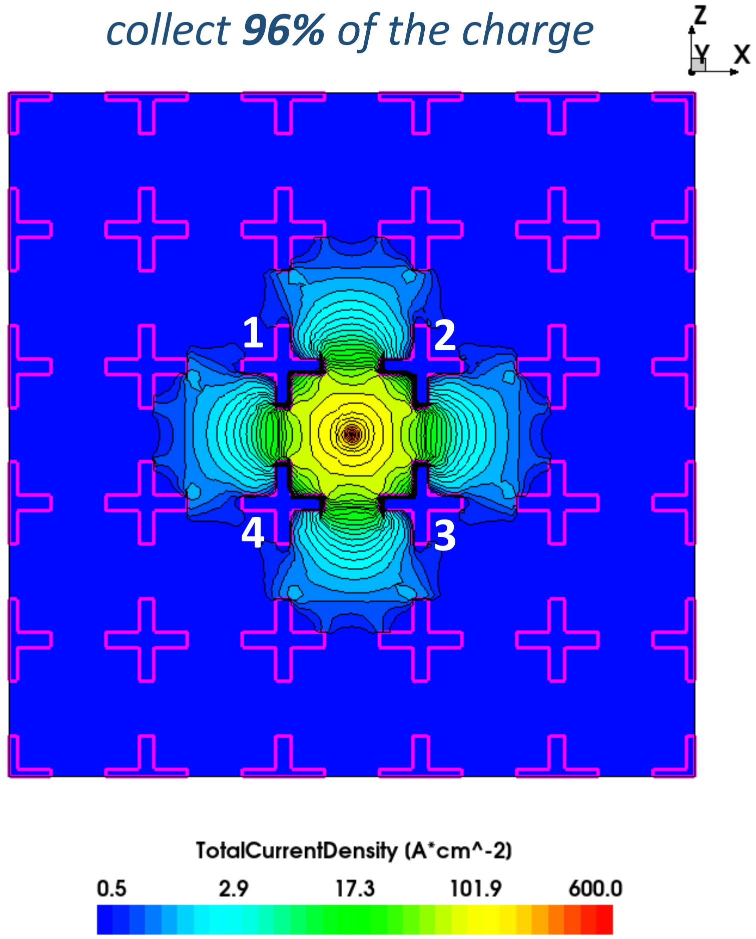

60 electrodes

*The four pads (1, 2, 3 and 4) collect **97%** of the charge*

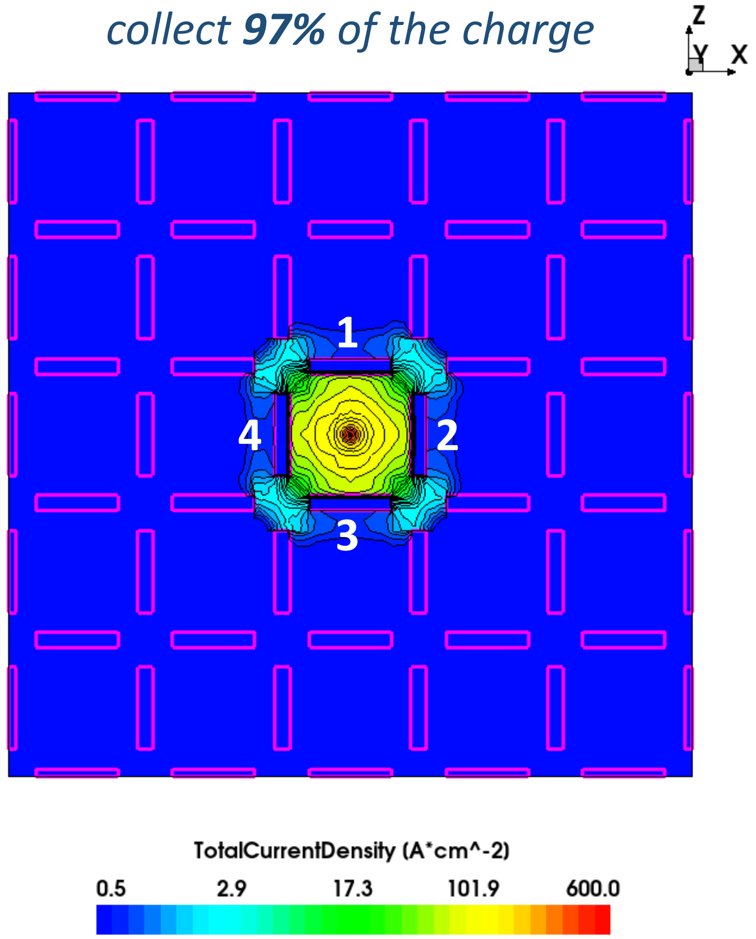

Playing with pad shape and dimension

Improving signal confinement: contact resistance

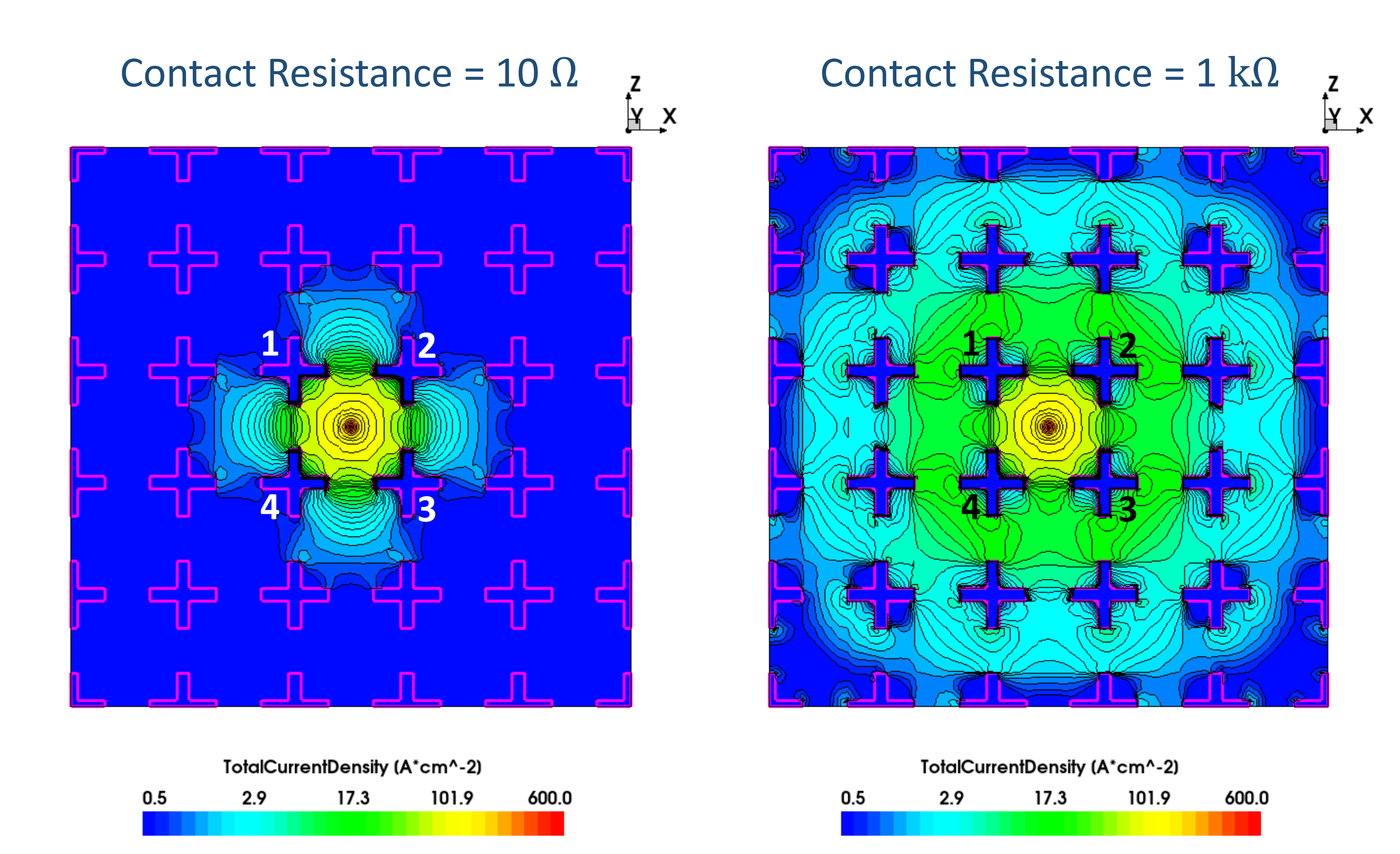

Resistive strips

Improving signal confinement

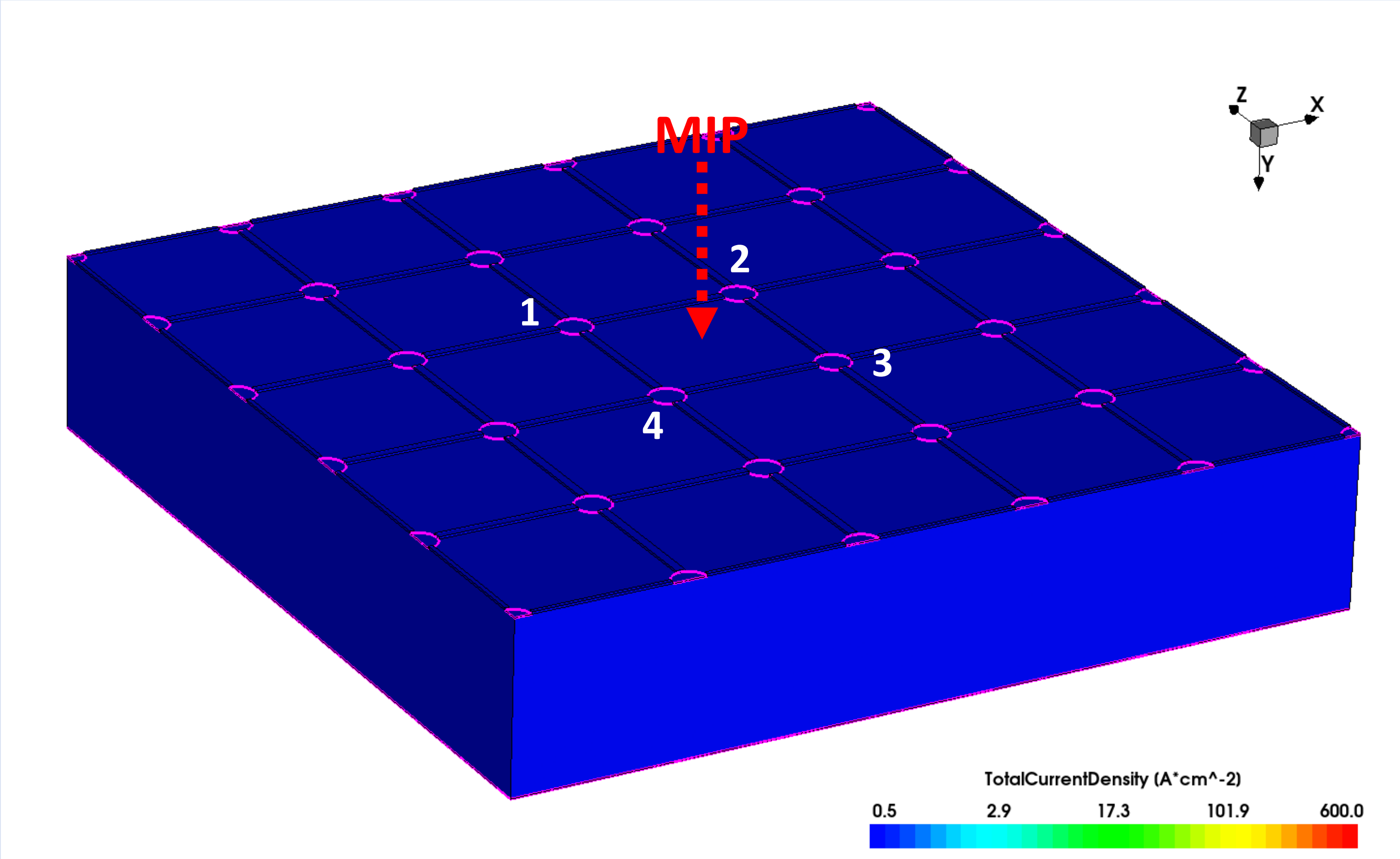

Low-impedance path among the collecting electrodes

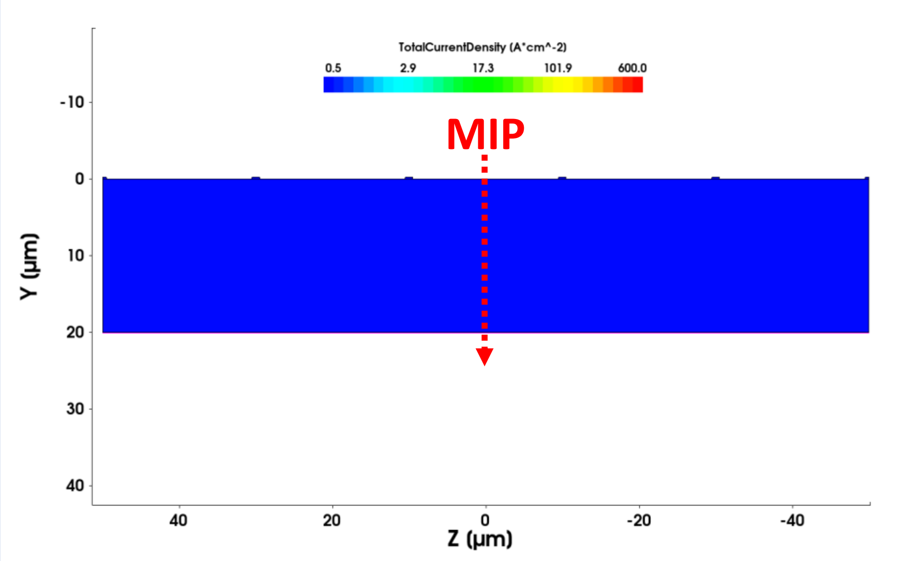

Resistive strips

Improving signal confinement: strip resistance tuning

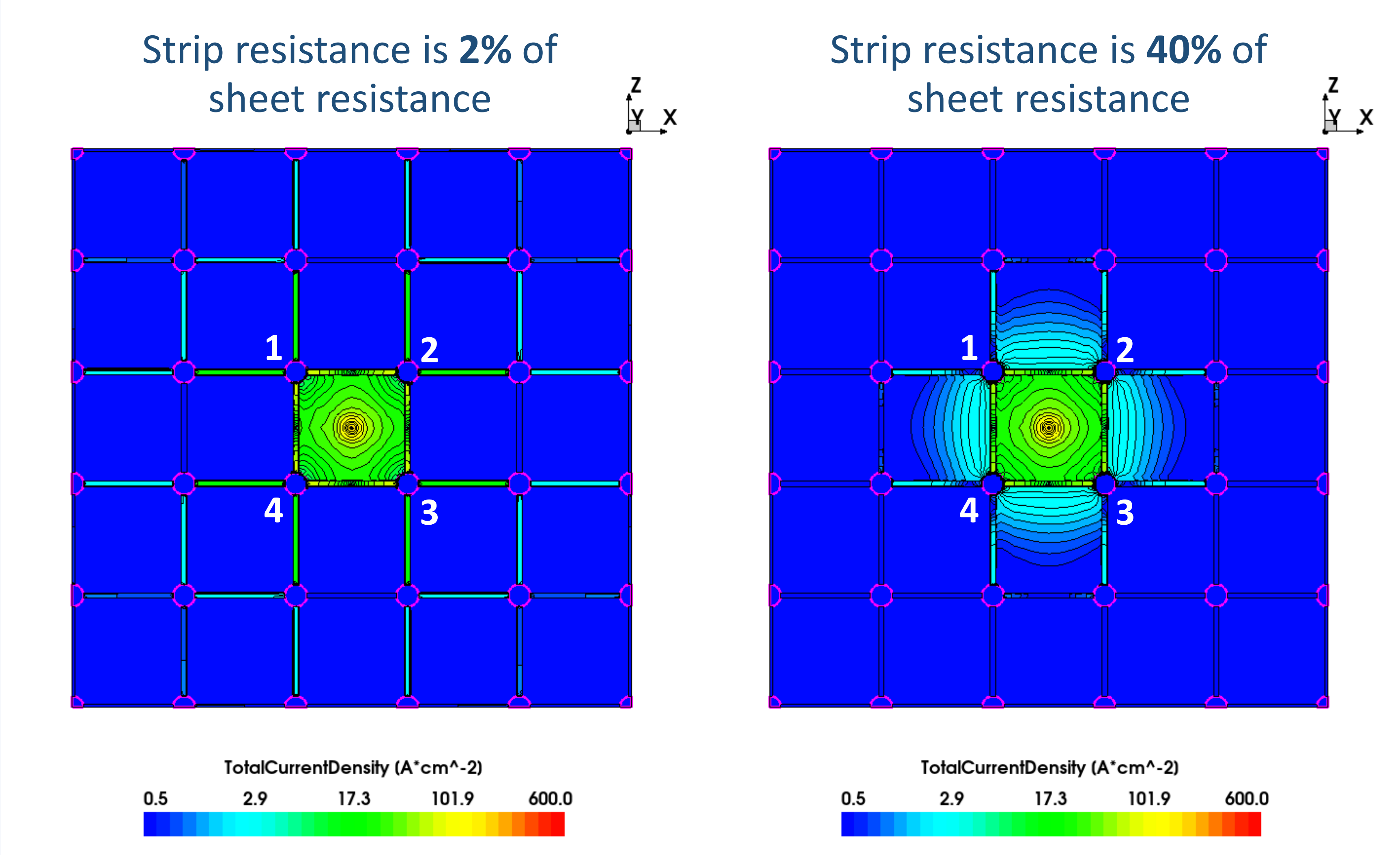

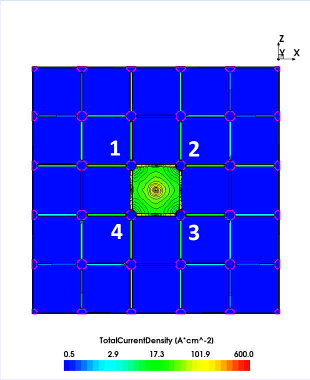

Resistive strips

Improving signal confinement: strip resistance tuning

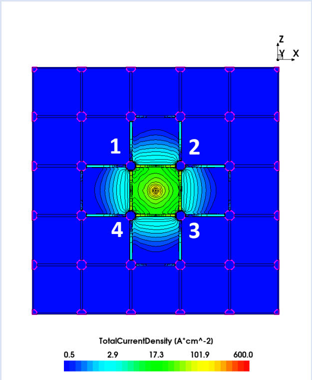

Strip resistance is **2%** of sheet resistance

Strip resistance is **40%** of sheet resistance

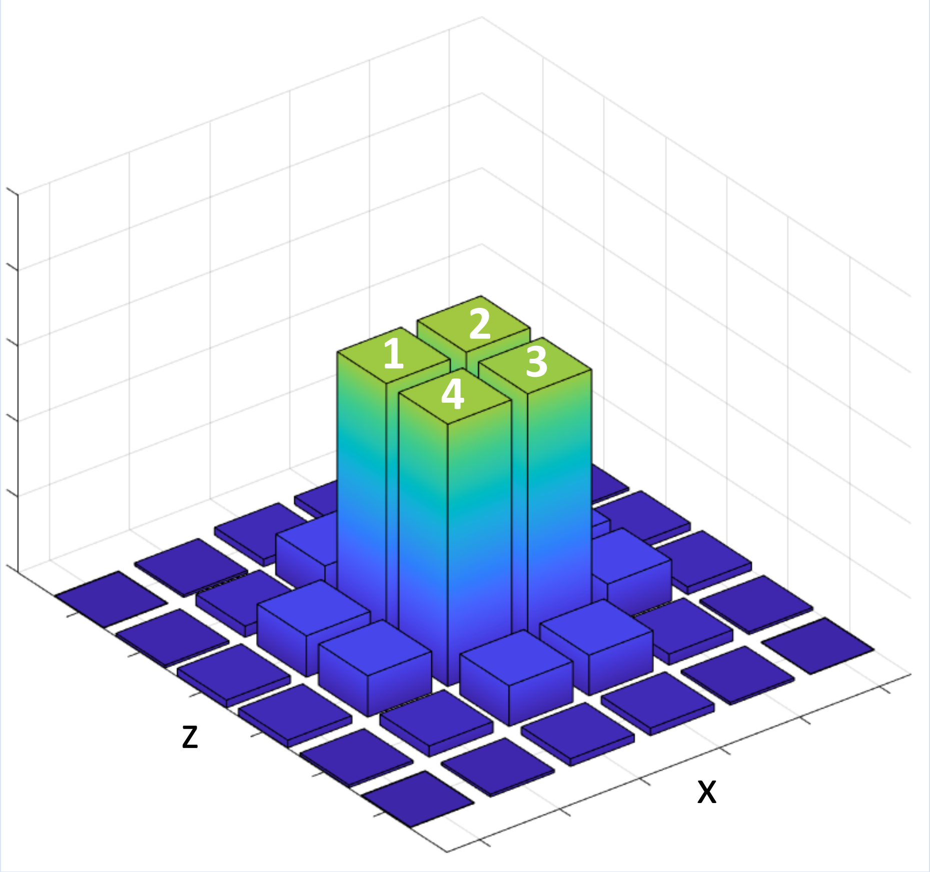

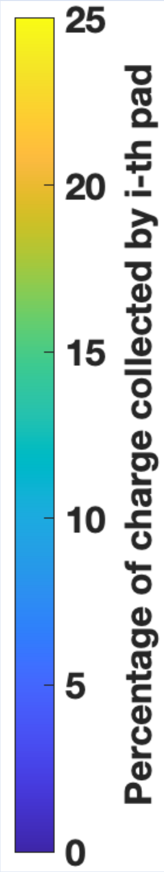

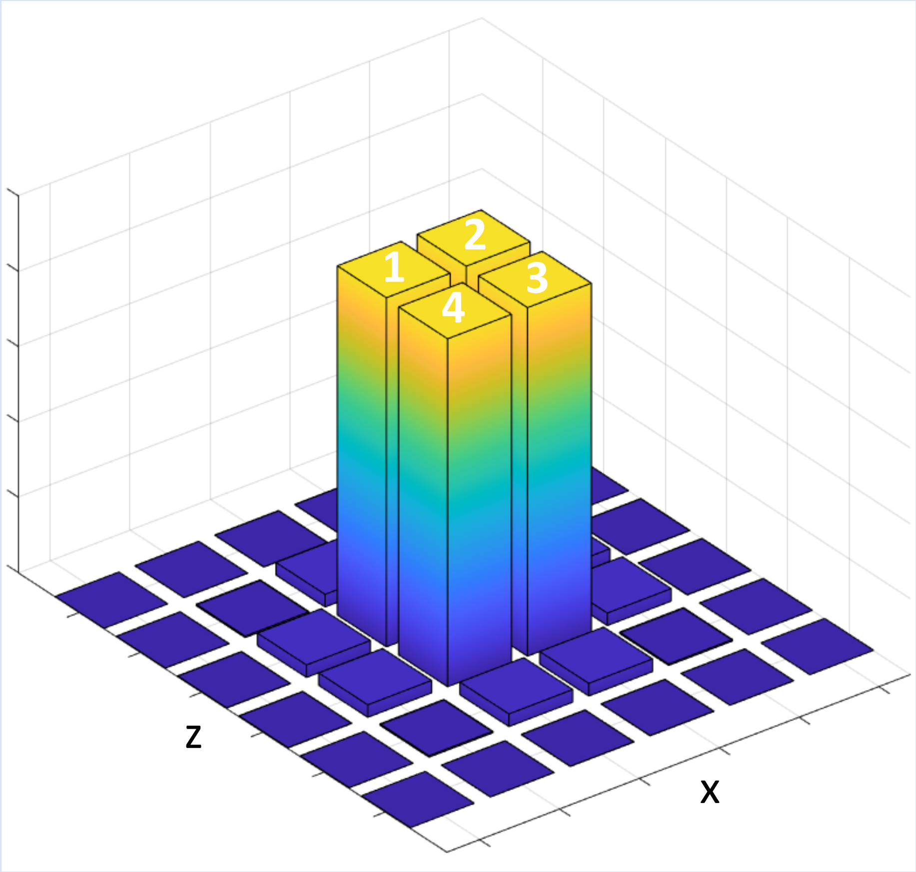

Silicon oxide trenches

Improving signal confinement

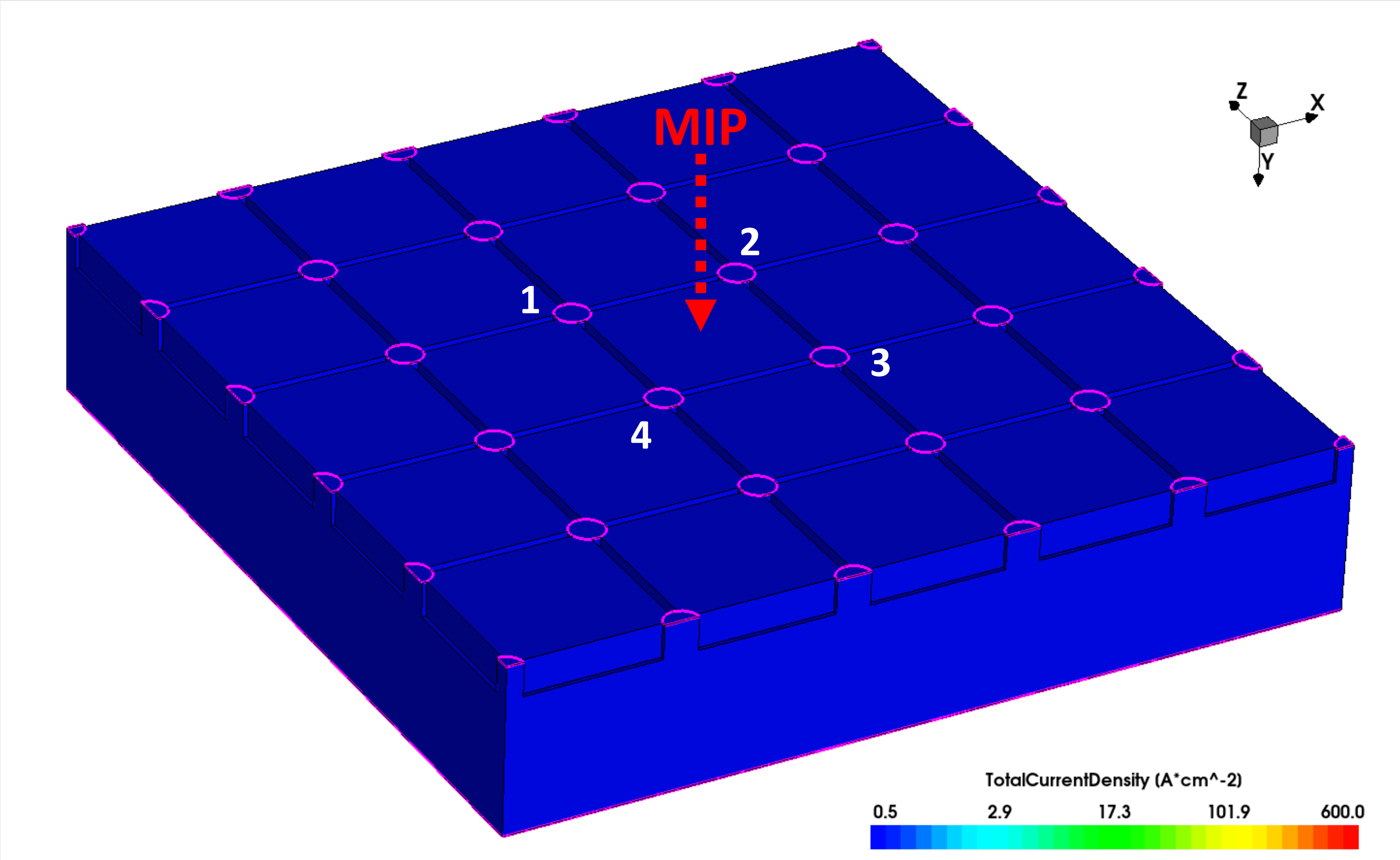

Interruption of the resistive path among neighbouring pixels

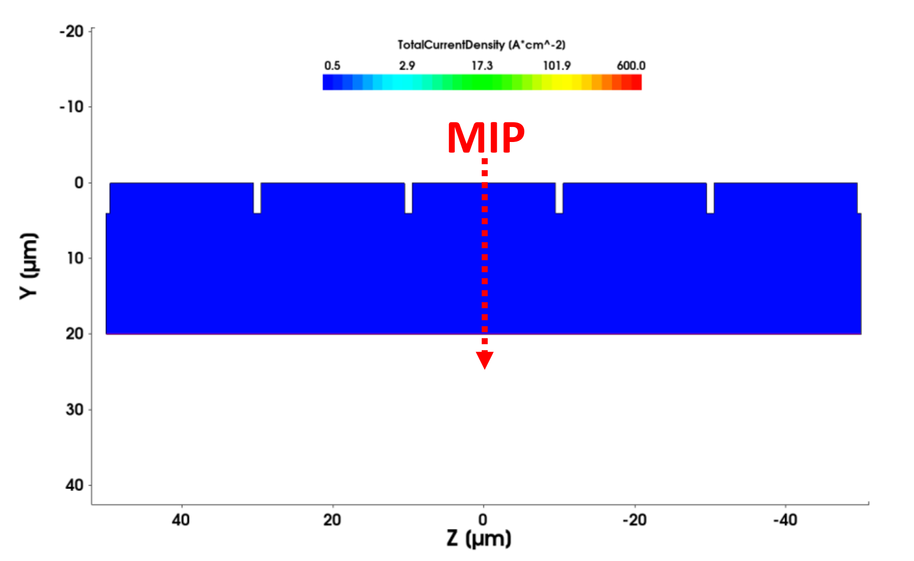

Silicon oxide trenches

Improving signal confinement: power of trenches

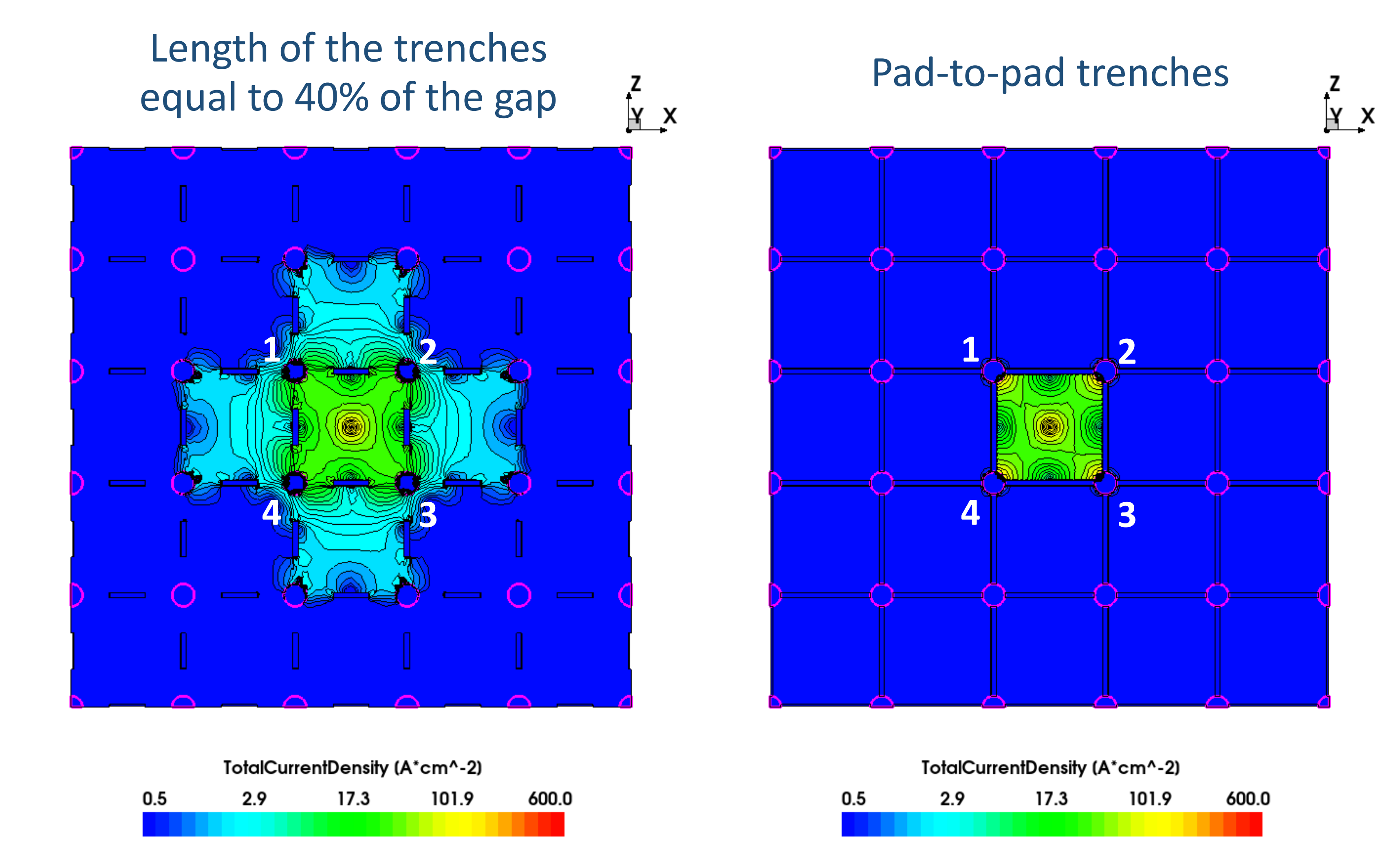

Silicon oxide trenches

Improving signal confinement: power of trenches

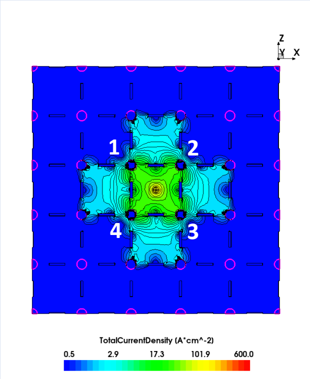

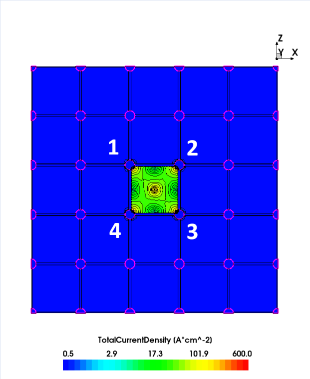

Length of the trenches equal to 40% of the gap

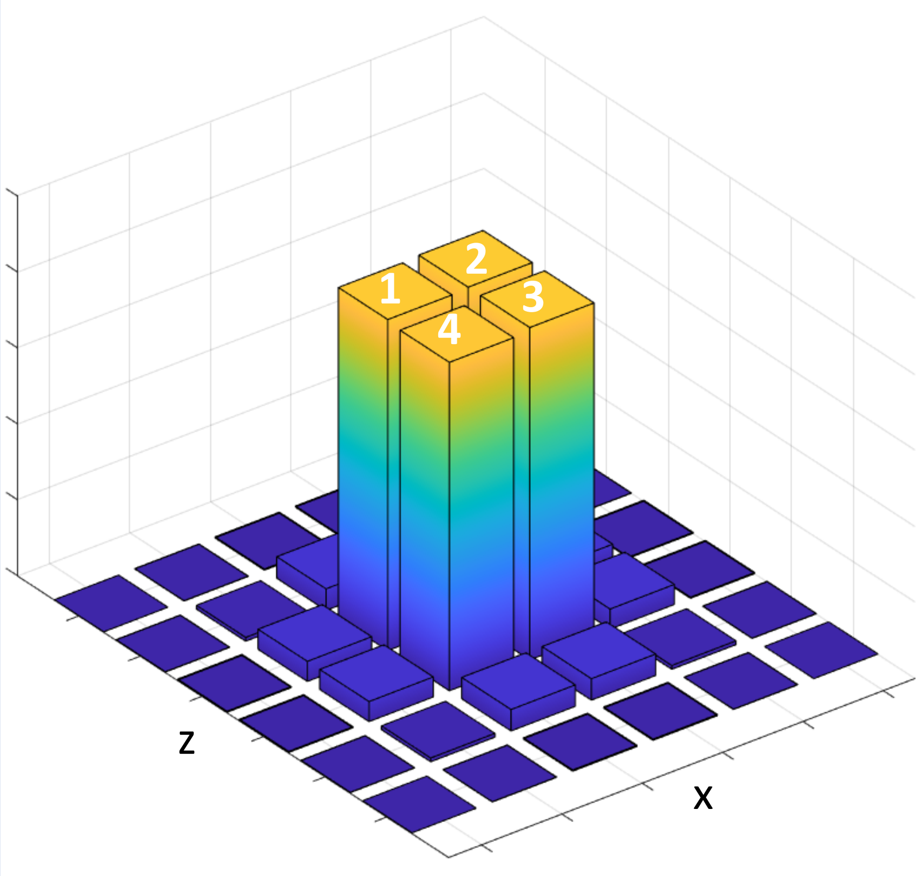

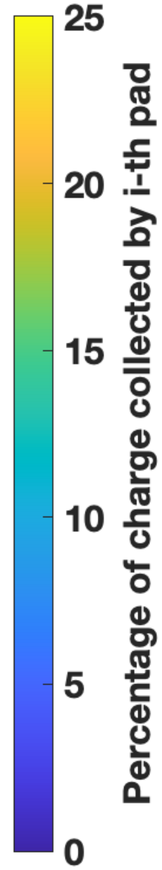

Pad-to-pad trenches

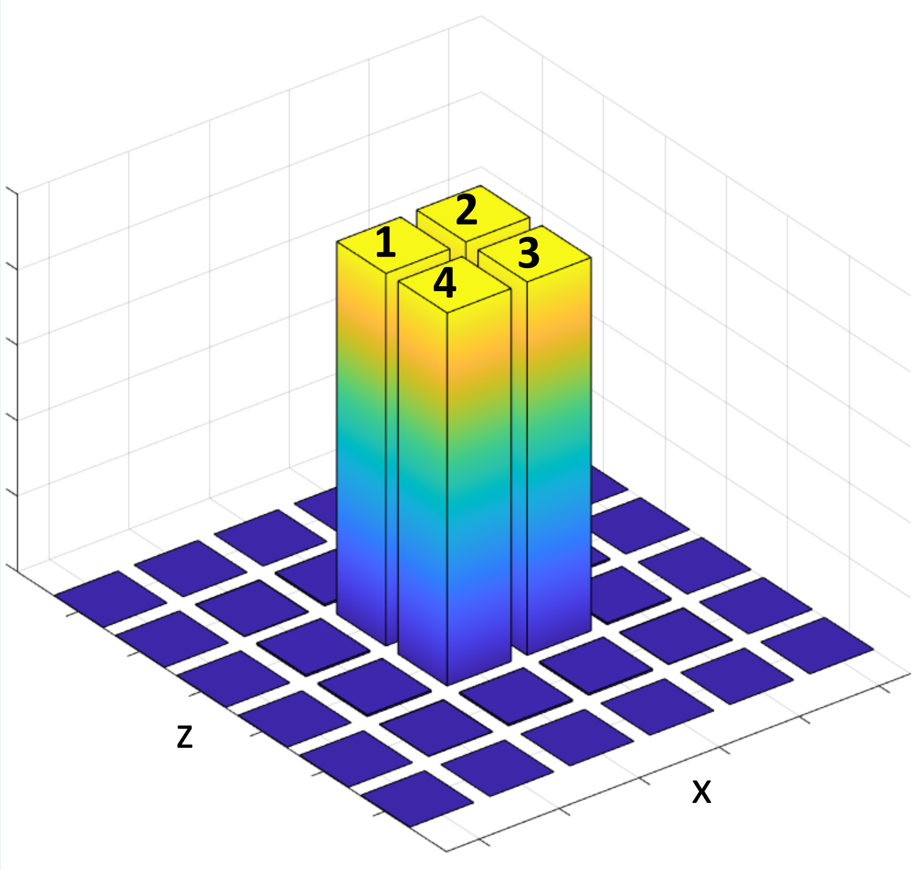

Conclusion

- Novel evolution of the LGAD-based Resistive Silicon Detector (RSD) design: DC-RSD
  - Overcoming of the drawbacks of the (AC-)RSDs by removing the dielectric and implanting the metal electrodes directly onto the n^+-resistive sheet.
- DC-RSD simulation strategy: two-step procedure, by combining Spice and TCAD simulation tools.
- The developed simulation framework enables quantitative evaluation of the effects of the technology realization (i.e., doping, geometry and material), geometrical layout, injected stimulus (MIP), and radiation-induced damage (UNIPG model) on the sensor behaviour.
- Guidelines for the first production of DC-RSD devices @ FBK (to be submitted in the summer)
  - use small electrodes to avoid introducing distortions in the reconstruction of the impact position;
  - trench interrupting the resistive n^+ layer excellently confines the signal;
  - resistive strips are also good at confining the signal, tuning of their resistance is important.

Thanks for your attention

Standard silicon pixel detector

To be achieved:

- Spatial resolution ~ $5\ \mu m$ ⇒ Lots of tiny pixels ⇓ Each one is a channel to read
- Very low power consumption ⇐ (✖) Each one is a channel to read

  Air cooling $< 0.2\ W/cm^2$

$$\sigma_s \sim \frac{Pitch}{\sqrt{12}}$$

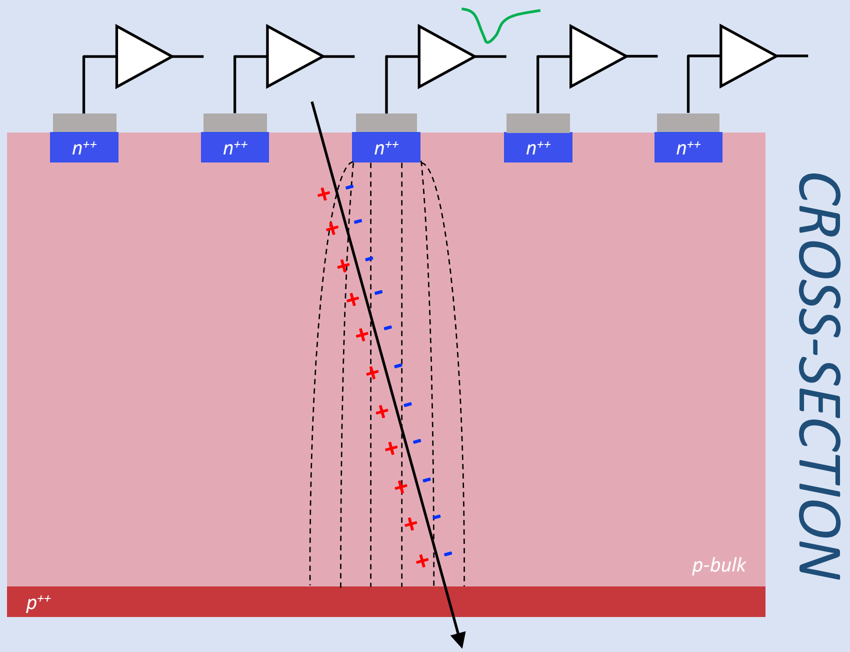

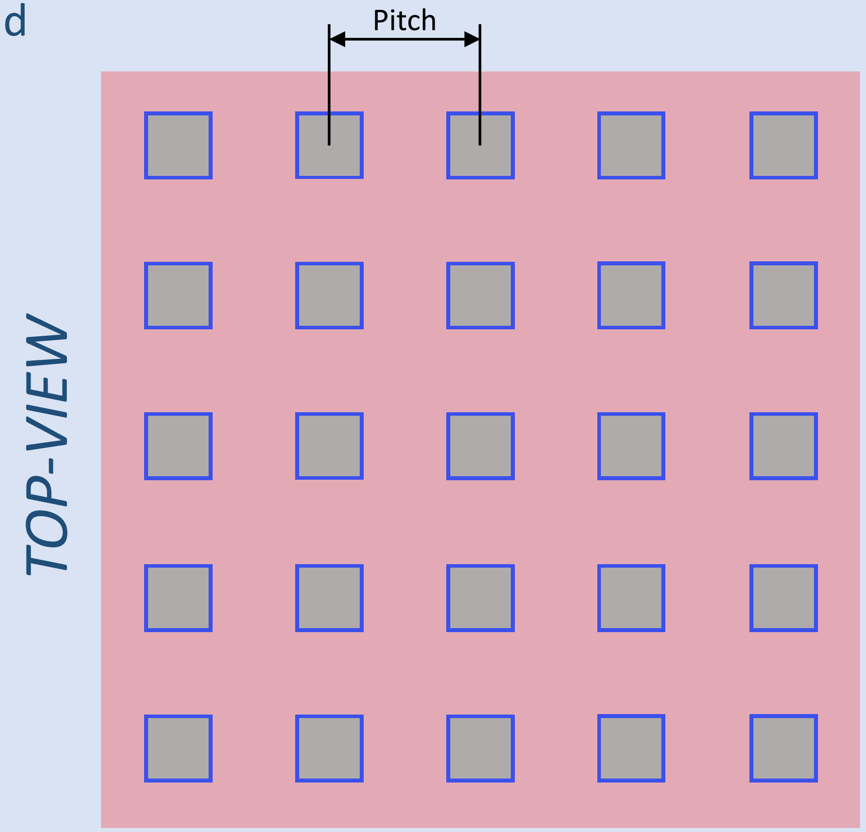

Resistive Silicon Detectors (RSDs)

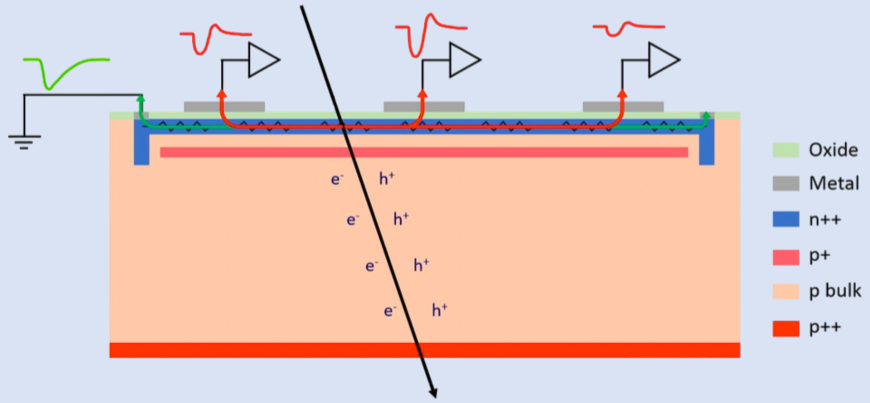

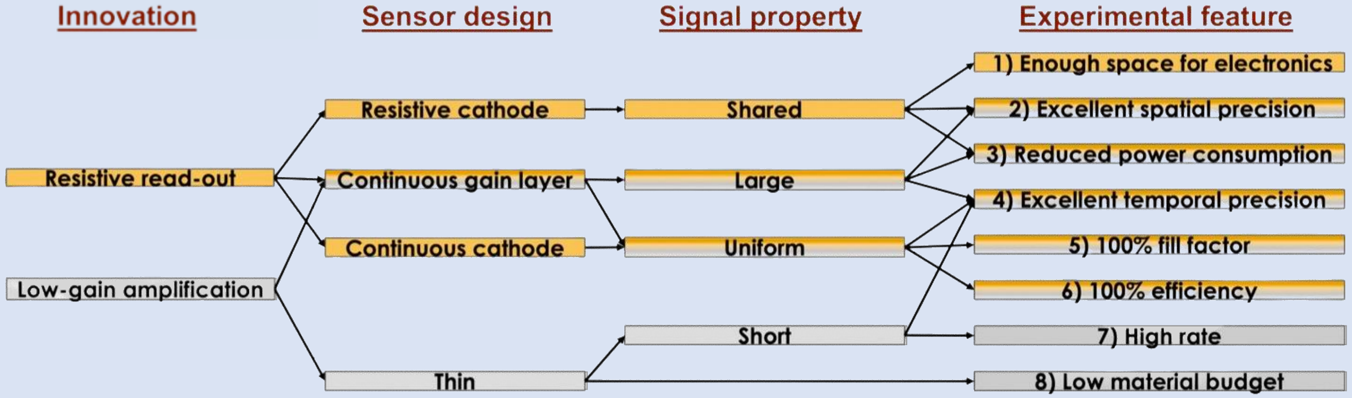

RSD2 production (FBK 2021)

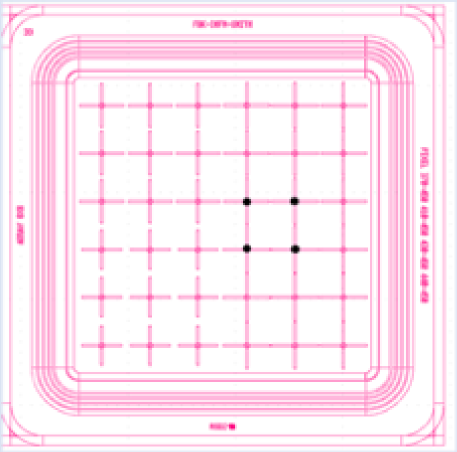

FONDAZIONE BRUNO KESSLER

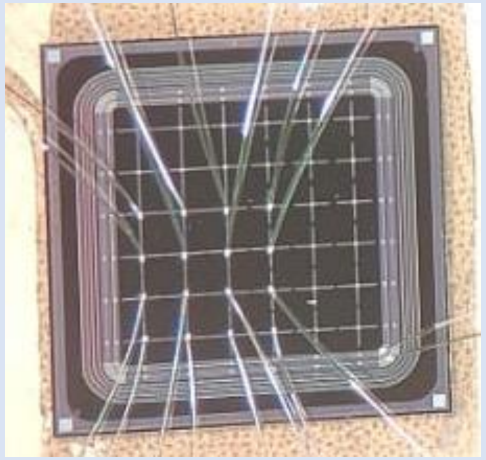

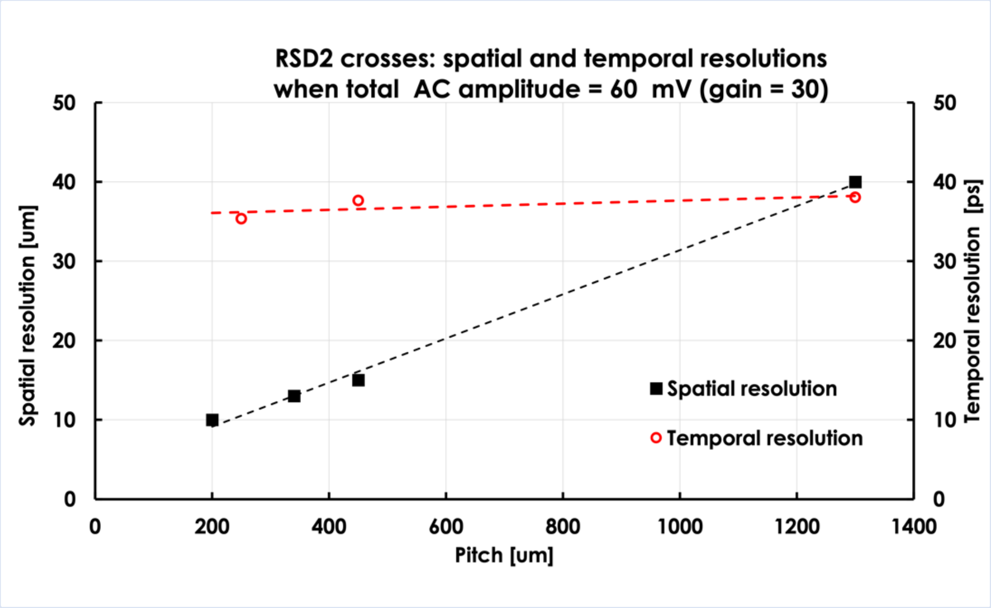

DC-RSD TCAD simulation: pitch
Distortion in the reconstruction of the particle impact position

NB: the maps obtained with Spice and TCAD simulations (Fig. 8 & Fig. 4) confirm that the reconstructed points tend to cluster in the centre of the pixel (four-pad cluster). Such distortion is typical of resistive devices [9]. By fixing the pad width, the larger the pitch size the higher the degree of the distortion (Fig. 8 vs. Fig. 9).

Fig. 5

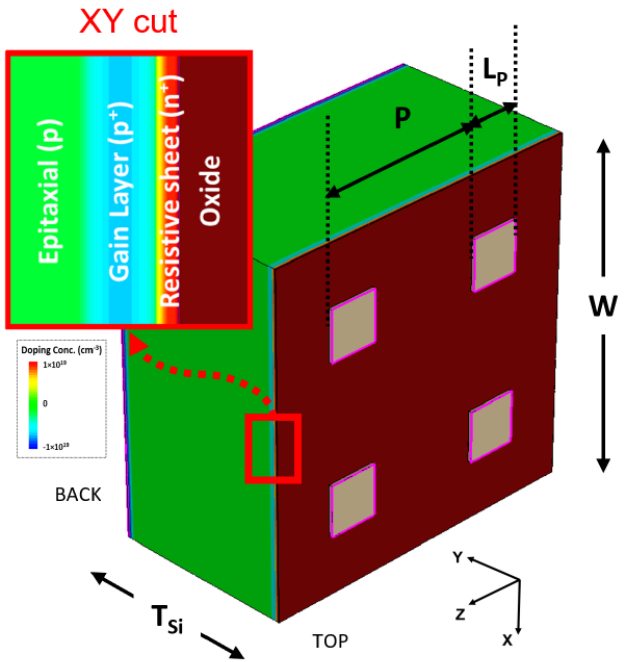

Fig. 9

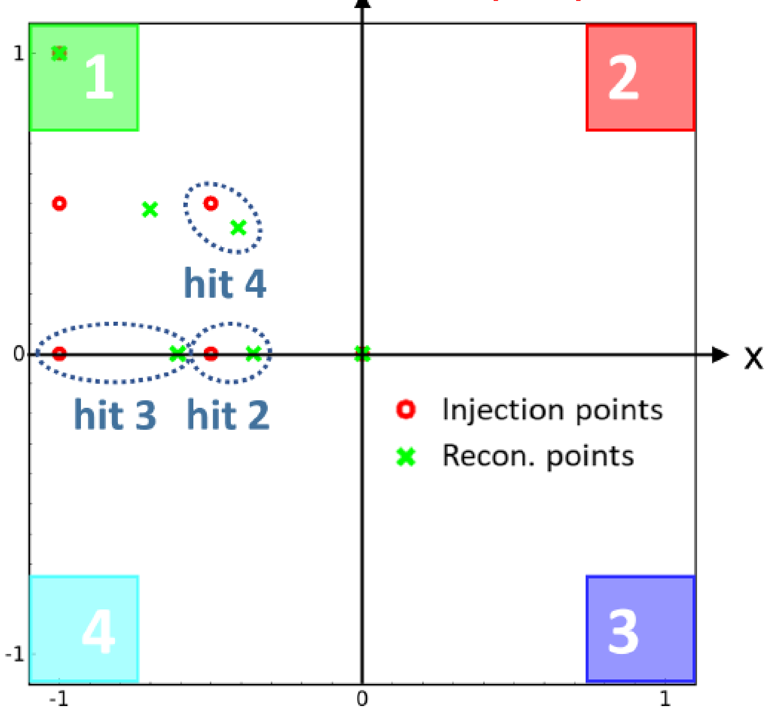

Fig. 8

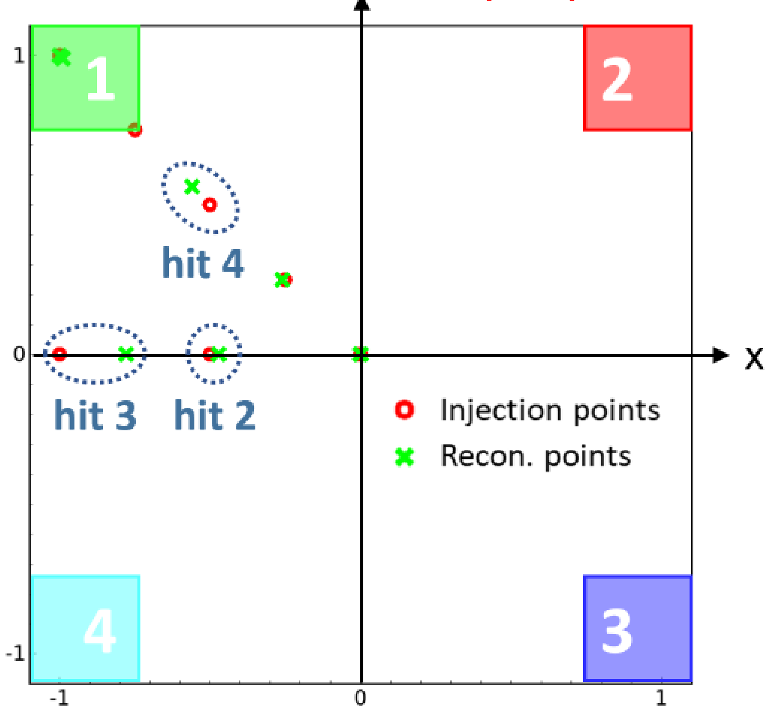

[9] H. Wagner *et al.*, On the dynamic two-dimensional charge diffusion of the interpolating readout structure employed in the MicroCAT detector, Nucl. Inst. and Meth. in Phys. Res. A, 482 (2002) 334.

A new design of resistive silicon detector: DC-RSD

Optimization: the map of the reconstructed impact positions (Fig. 12) shows a better accuracy of the position reconstruction in the case of DC-RSD flavour characterized by strip-connected pads (blue diamond markers), because they help to confine the signal spreading within the pixel (Fig. 11).

Fig. 10

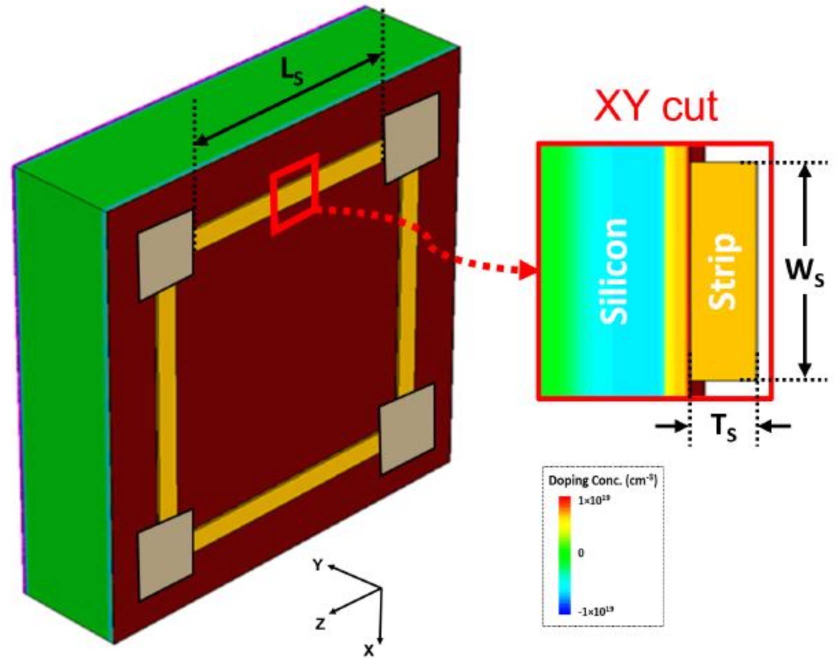

Fig. 11

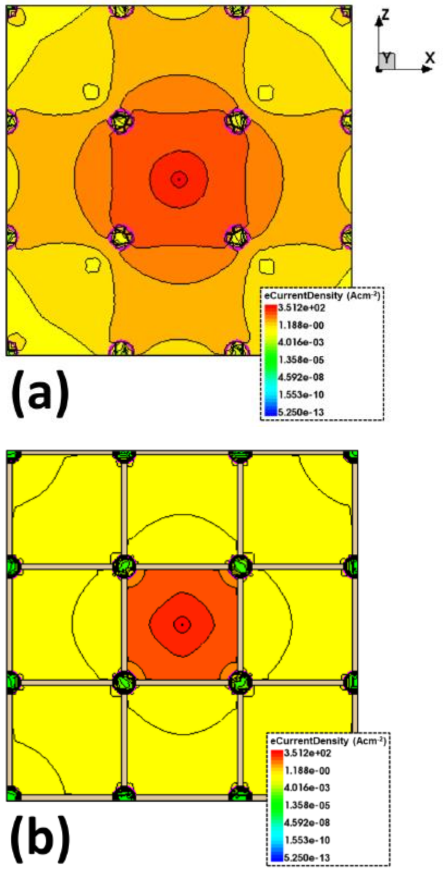

Fig. 12

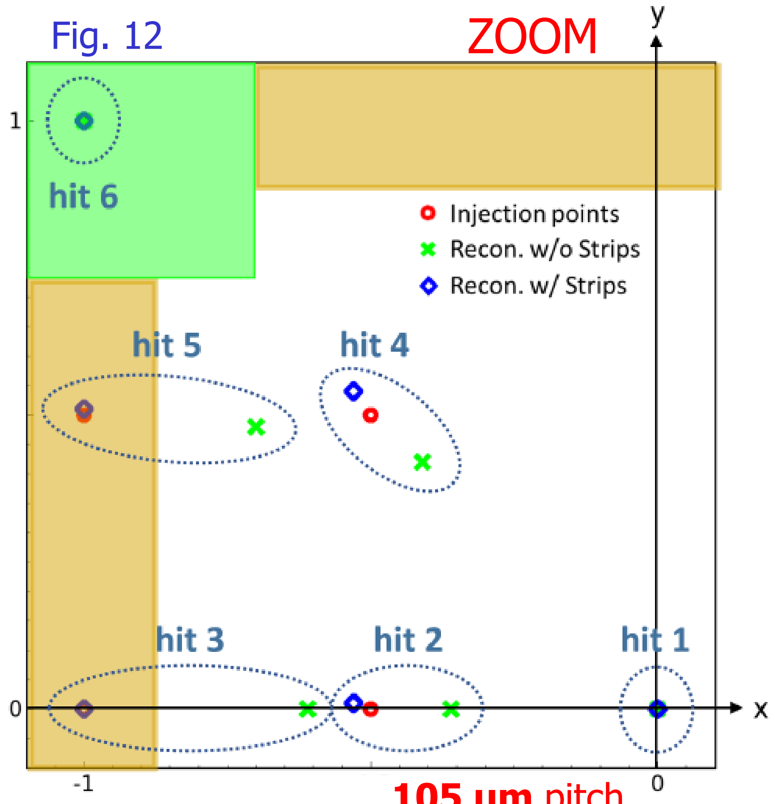

A new design of resistive silicon detector: DC-RSD

Optimization: evaluation of the impact of different values of the strip resistance on the transient behaviour (Fig. 13) and the reconstruction of the particle impact positions (Fig. 14).

Fig. 13

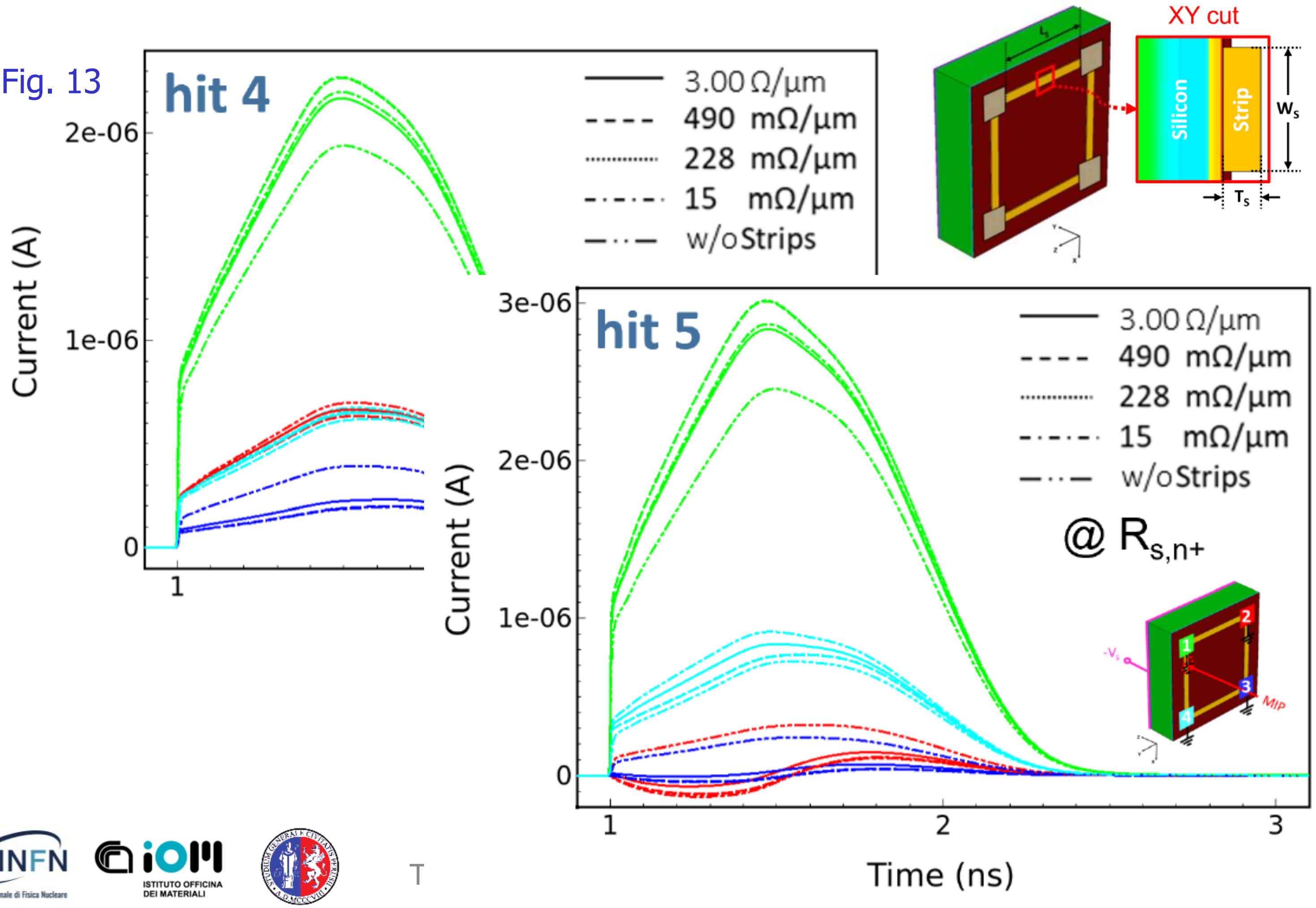

Fig. 14

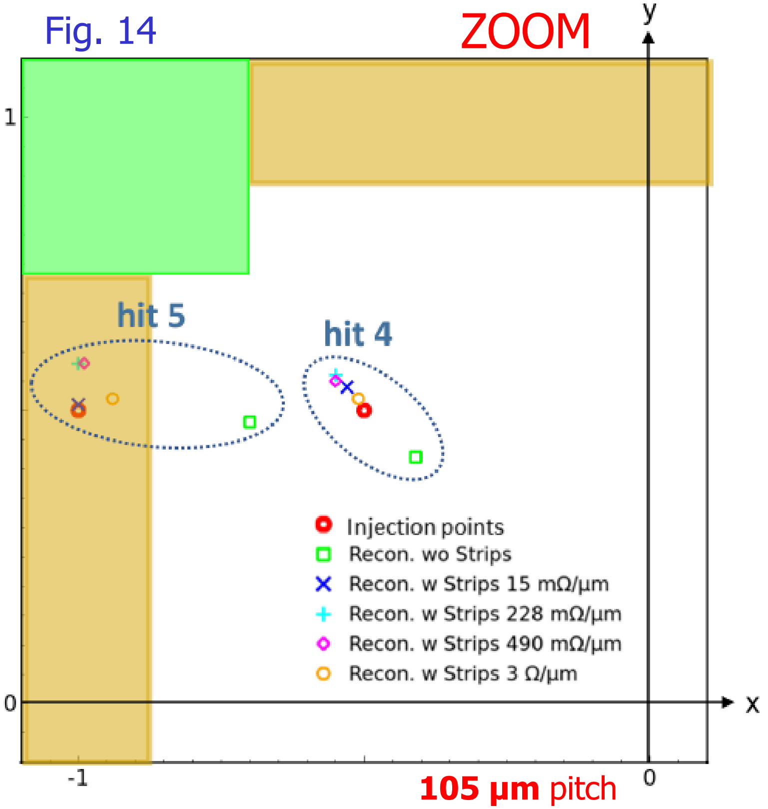

105 µm pitch
1 kΩ/sq R_{sheet}

A new design of resistive silicon detector: DC-RSD

Optimization: evaluation of the impact of different values of the pad width on the transient behaviour (Fig. 15) and the reconstruction of the particle impact positions (Fig. 16).

Fig. 15

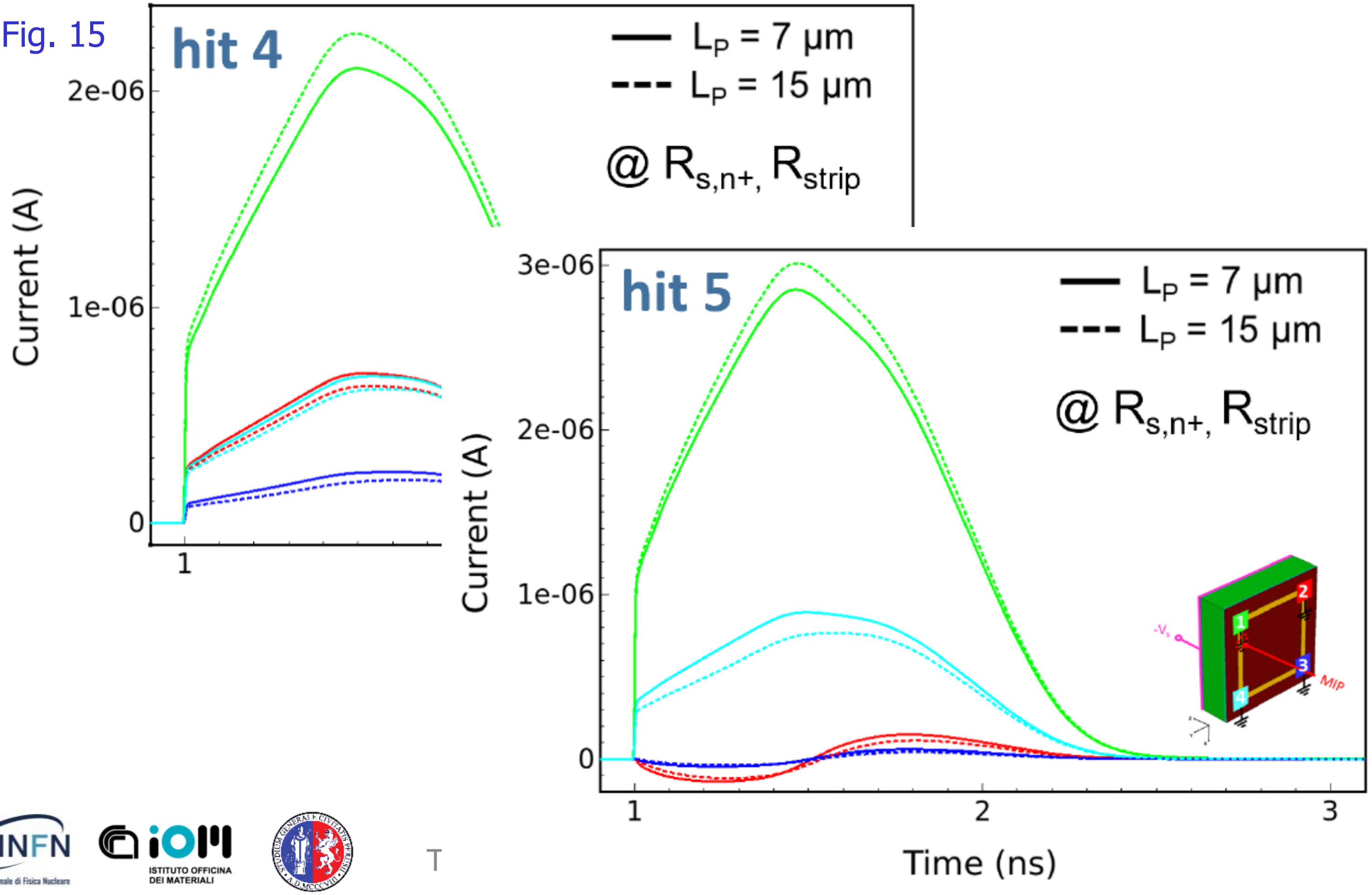

Fig. 16

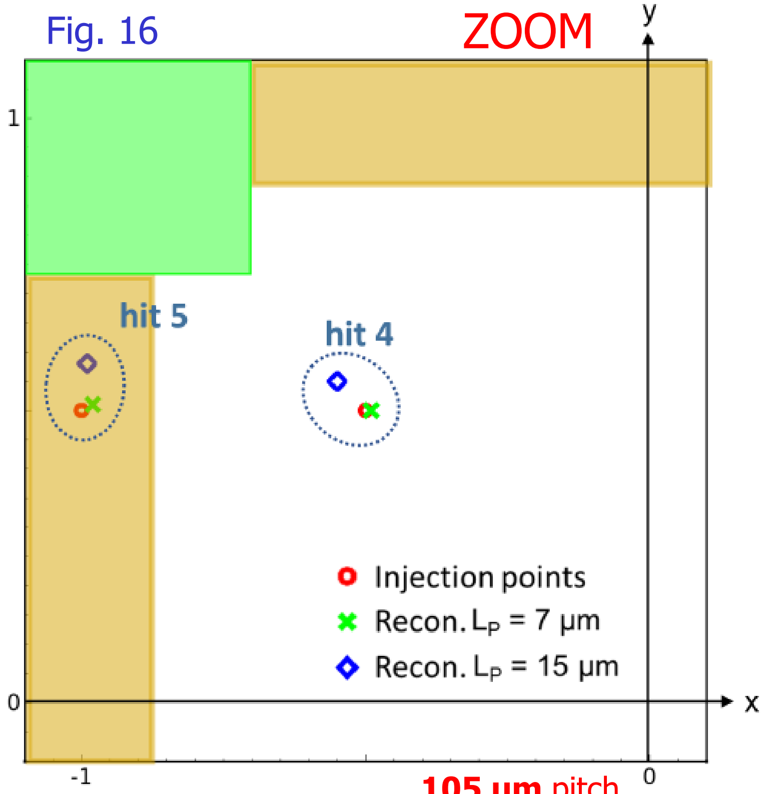

105 μm pitch
1 kΩ/sq R_{sheet}, **1 Ω/μm** R_{strip}

tommaso.croci@pg.infn.it

A new design of resistive silicon detector: DC-RSD

Guidelines for the DC-RSD production @ FBK:

- The need of having signal spreading contained within a limited set of pads (preferably four) to not get worse the spatial resolution fixes a **lower limit** of the **sheet resistance** value of about **1 kΩ/sq**, which also ensures the electrical isolation between the pads.
- When tuning the value of the sheet resistance (i.e., by varying the thickness of the n^+-resistive sheet) it is important to consider a proper shaping of the gain layer implant to avoid the early breakdown of the device.
- A reasonable **lower limit** for the **pitch** size is of about **100 μm** to have a good compromise between the reconstruction of the particle impact positions and the number of readout channels.
- The accuracy of the reconstruction of the particle impact positions improves by using low-resistive strips between the read-out electrodes, because they help to confine the signal spreading within the pixel (i.e., a cluster of four pads).
- Fine-tuning of the **strip resistance** (i.e., geometry and material) such that it is lower than the sheet resistance, but not enough to short circuit the front-end electronics. In particular: a **lower limit** of the strip resistance of about **1 Ω/μm** in the case of 100 μm-pitch sensor ensures that the total resistance of the strip is higher than the input impedance of the amplifiers (i.e., 50 Ω).
- A reasonable **lower limit** for the **pad size** is of about **10 μm** for a 100 μm-pitch sensor.

Reconstruction of the impact coordinates

Centre-of-gravity method (charge)

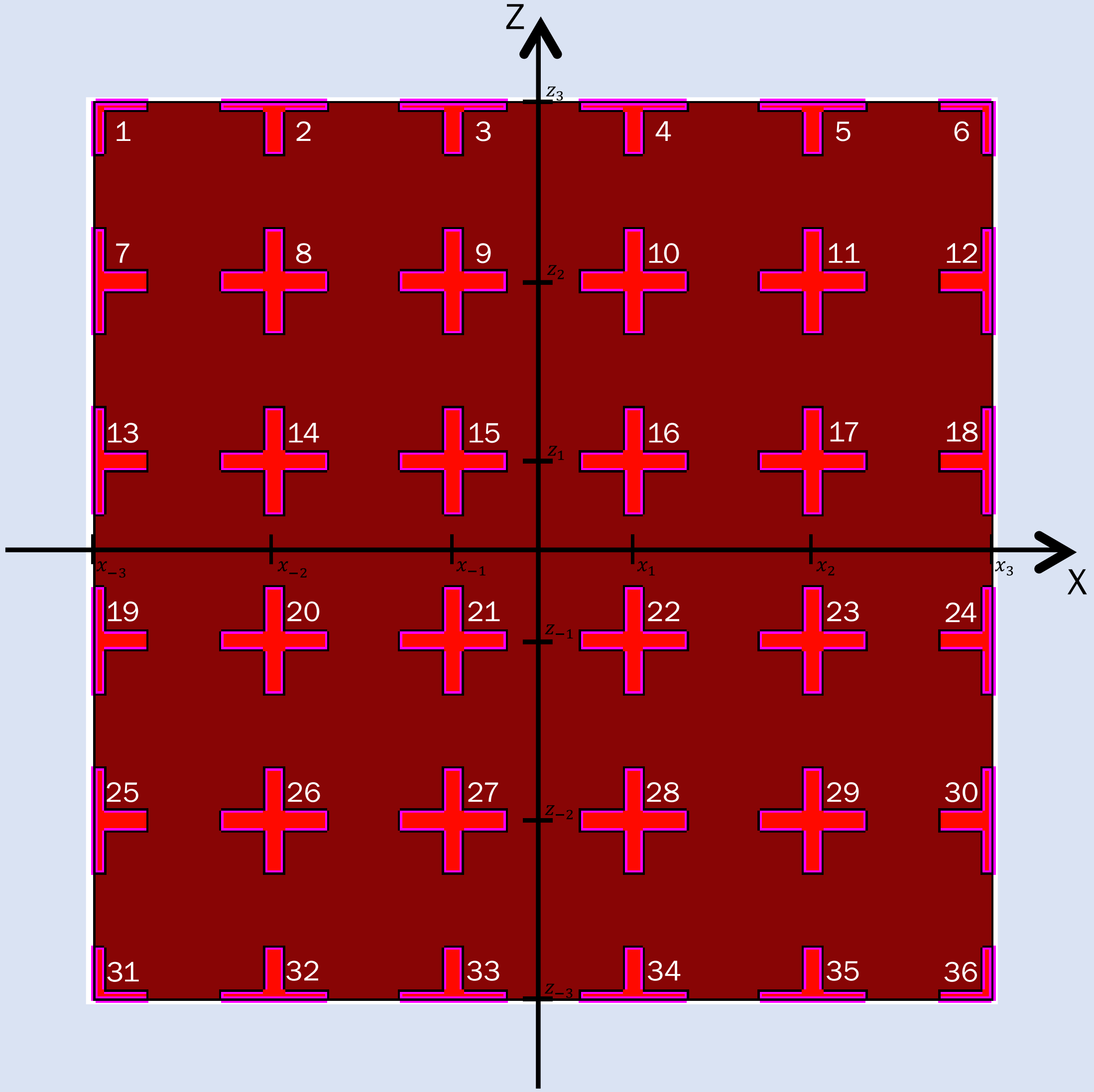

X-coordinate

- $Q_{x_{-3}} = Q_1 + Q_7 + Q_{13} + Q_{19} + Q_{25} + Q_{31}$
- $Q_{x_{-2}} = Q_2 + Q_8 + Q_{14} + Q_{20} + Q_{26} + Q_{32}$
- $Q_{x_{-1}} = Q_3 + Q_9 + Q_{15} + Q_{21} + Q_{27} + Q_{33}$
- $Q_{x_1} = Q_4 + Q_{10} + Q_{16} + Q_{22} + Q_{28} + Q_{34}$
- $Q_{x_2} = Q_5 + Q_{11} + Q_{17} + Q_{23} + Q_{29} + Q_{35}$
- $Q_{x_3} = Q_6 + Q_{12} + Q_{18} + Q_{24} + Q_{30} + Q_{36}$

$$X_R = \frac{\sum_{\substack{i=-3 \\ i\neq 0}}^{3} Q_{x_i} \cdot x_i}{\sum_{i=1}^{36} Q_i}$$

Z-coordinate

- $Q_{z_{-3}} = Q_{31} + Q_{32} + Q_{33} + Q_{34} + Q_{35} + Q_{36}$
- $Q_{z_{-2}} = Q_{25} + Q_{26} + Q_{27} + Q_{28} + Q_{29} + Q_{30}$
- $Q_{z_{-1}} = Q_{19} + Q_{20} + Q_{21} + Q_{22} + Q_{23} + Q_{24}$
- $Q_{z_1} = Q_{13} + Q_{14} + Q_{15} + Q_{16} + Q_{17} + Q_{18}$
- $Q_{z_2} = Q_7 + Q_8 + Q_9 + Q_{10} + Q_{11} + Q_{12}$
- $Q_{z_3} = Q_1 + Q_2 + Q_3 + Q_4 + Q_5 + Q_6$

$$Z_R = \frac{\sum_{\substack{i=-3 \\ i\neq 0}}^{3} Q_{z_i} \cdot z_i}{\sum_{i=1}^{36} Q_i}$$

Improving signal confinement

Resistive strips

Strip resistance is 40% of sheet resistance

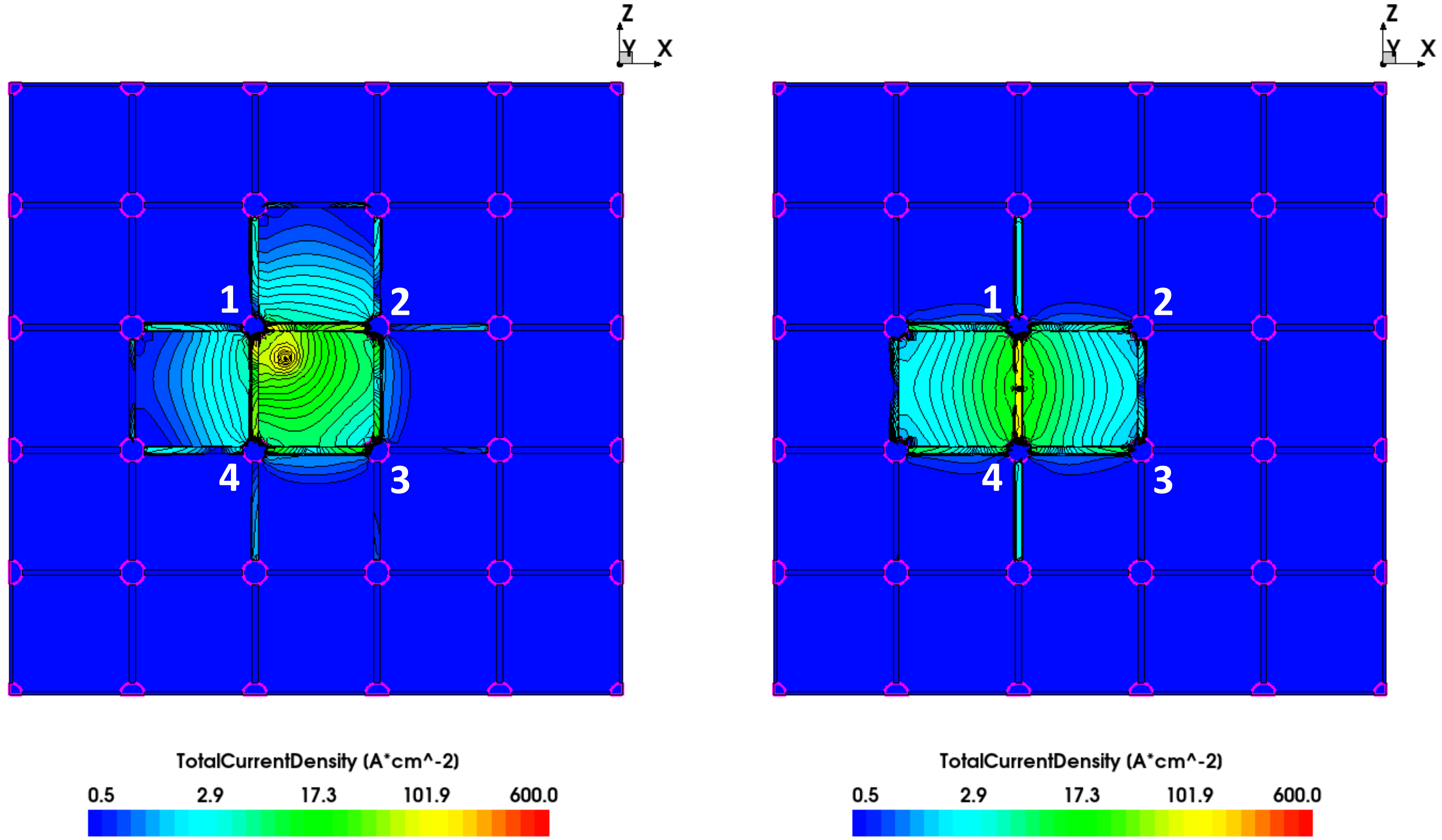

Resistive strips

Improving signal confinement

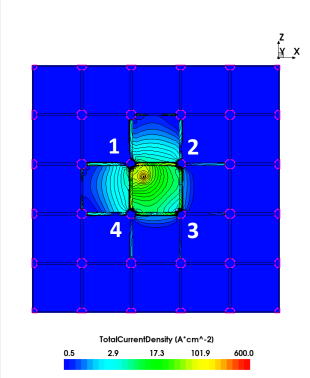

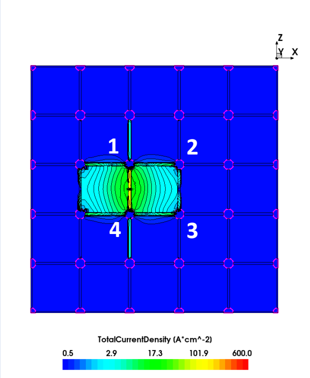

Strip resistance is **40%** of sheet resistance

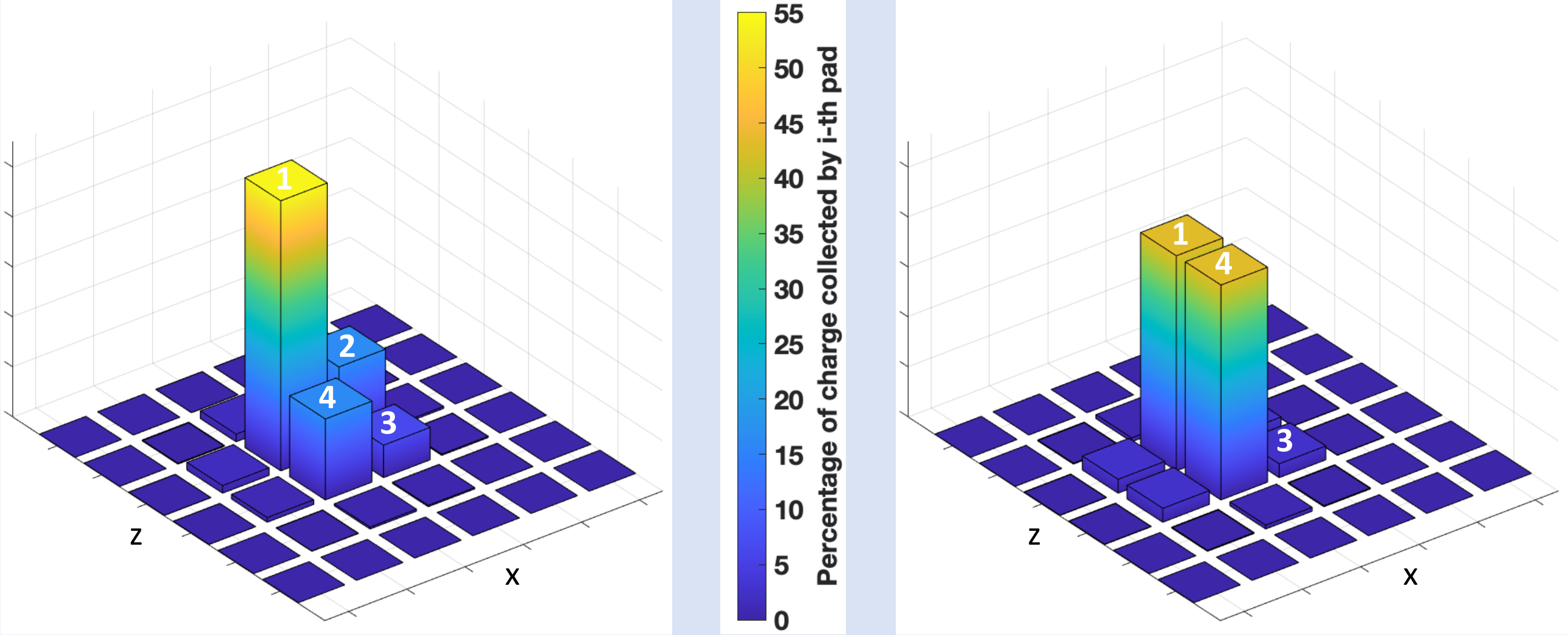

Improving signal confinement

Silicon oxide trenches

Pad-to-pad trenches

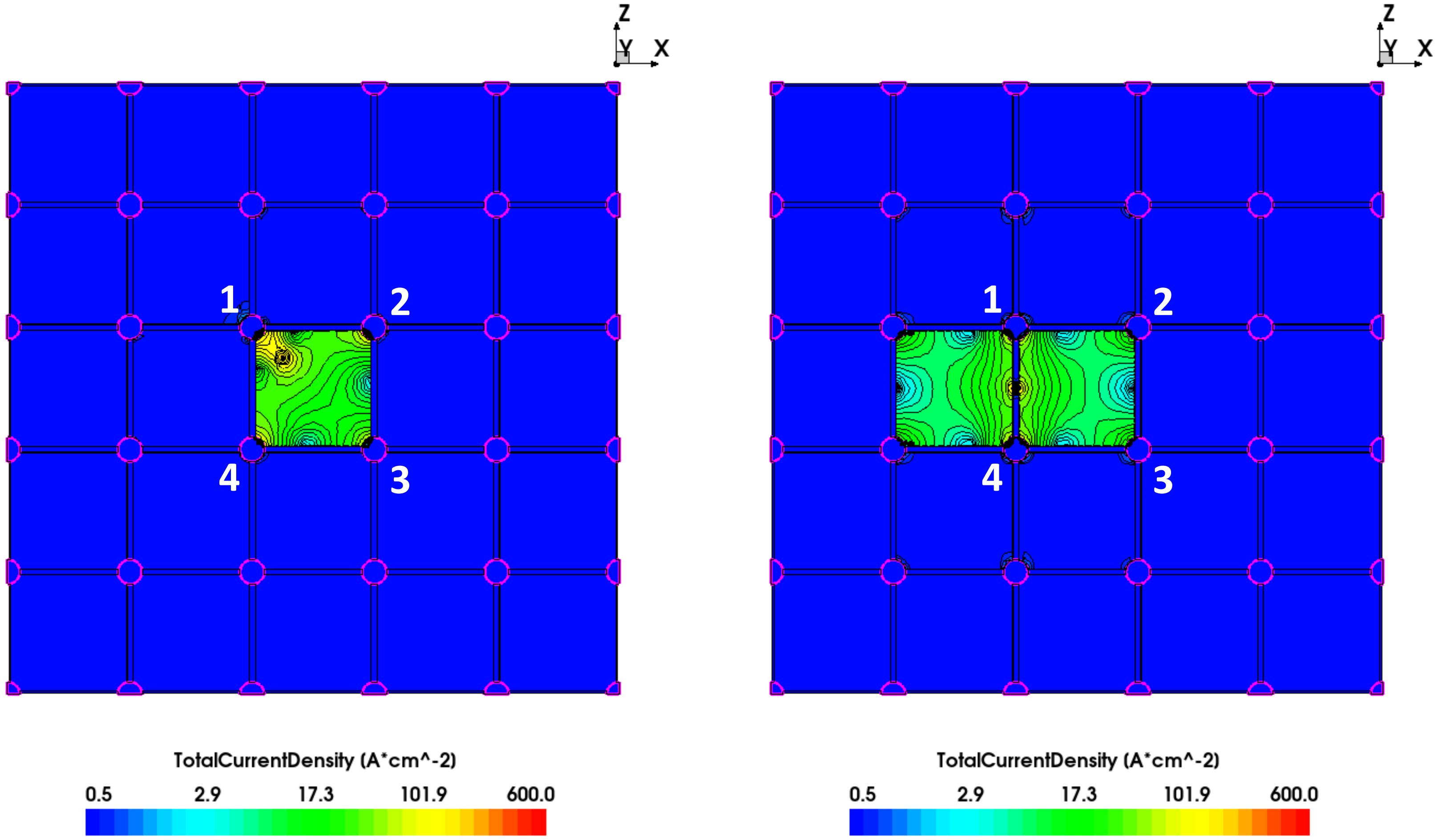

Silicon oxide trenches

Improving signal confinement

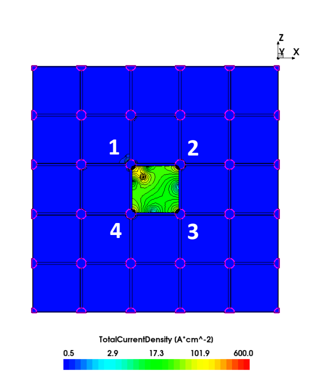

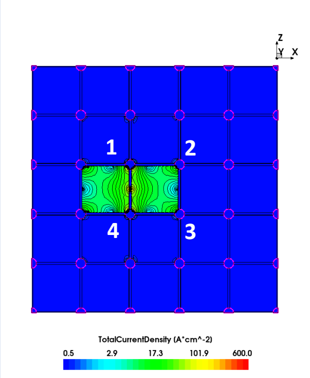

Pad-to-pad trenches

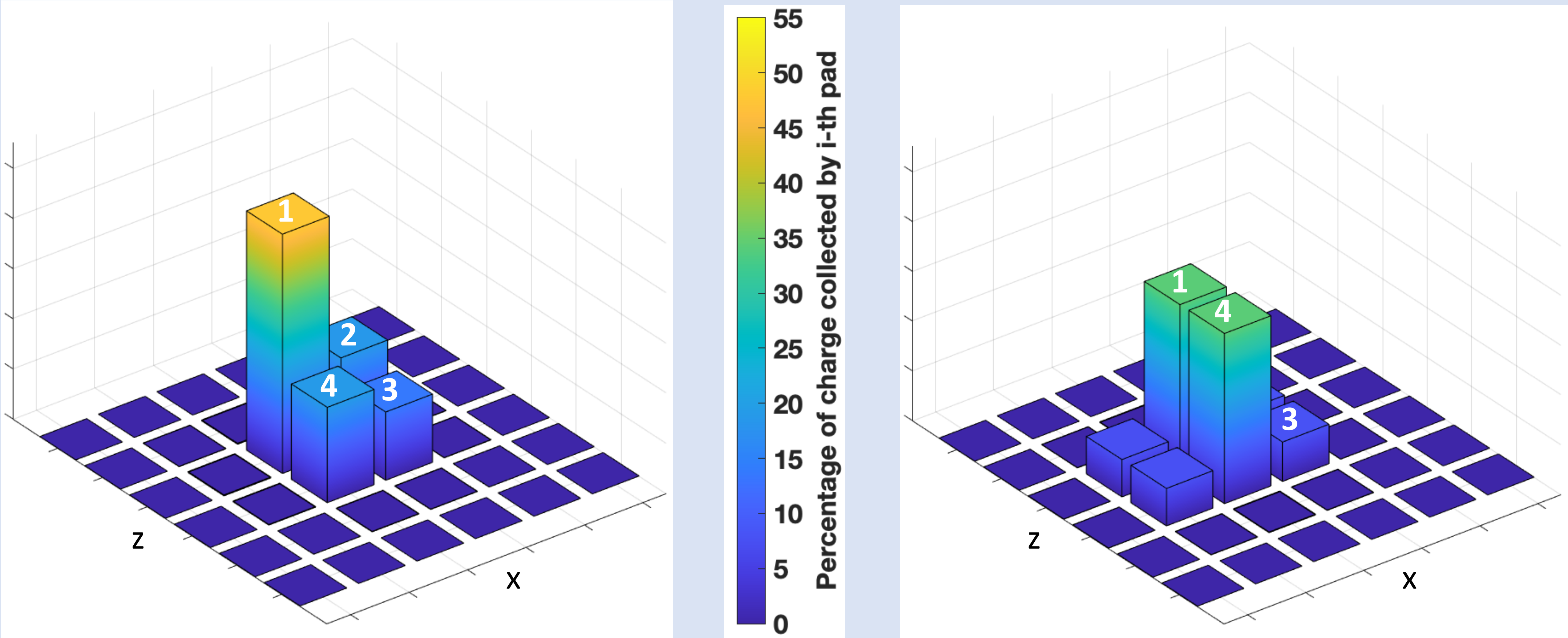

Strips vs. Trenches

Improving signal confinement

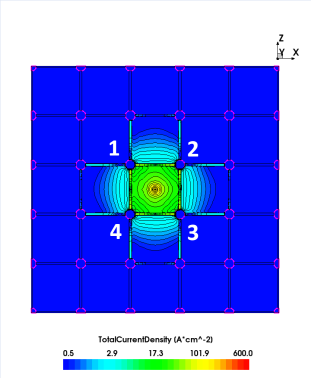

Strip resistance is **40%** of sheet resistance

Pad-to-pad trenches

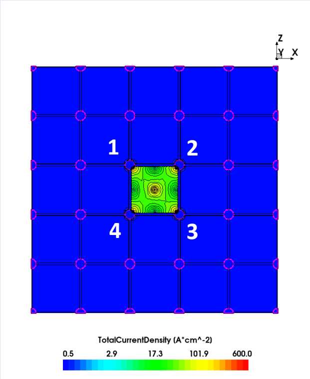

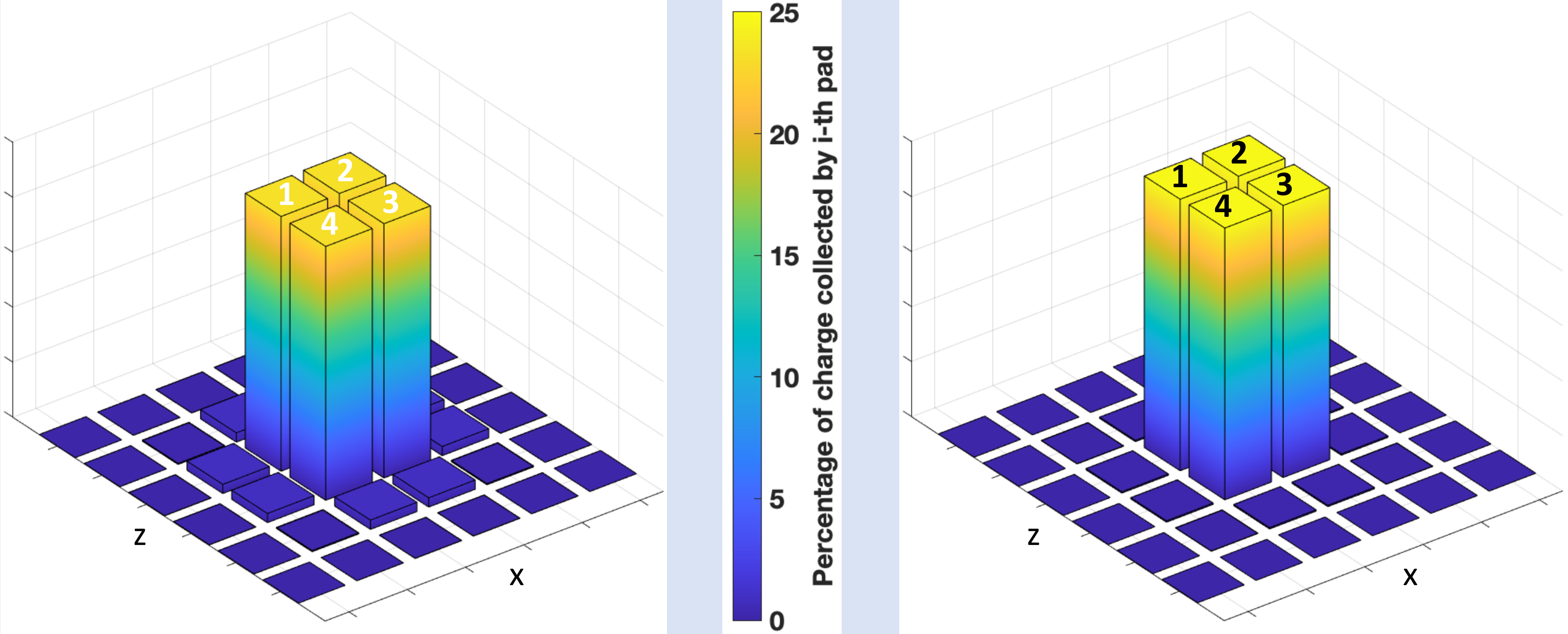

Strips vs. Trenches

Improving signal confinement

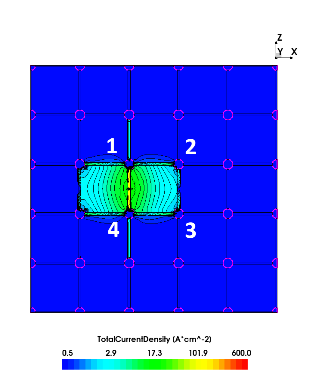

Strip resistance is **40%** of sheet resistance

Pad-to-pad trenches

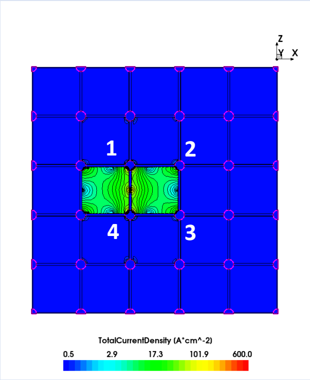

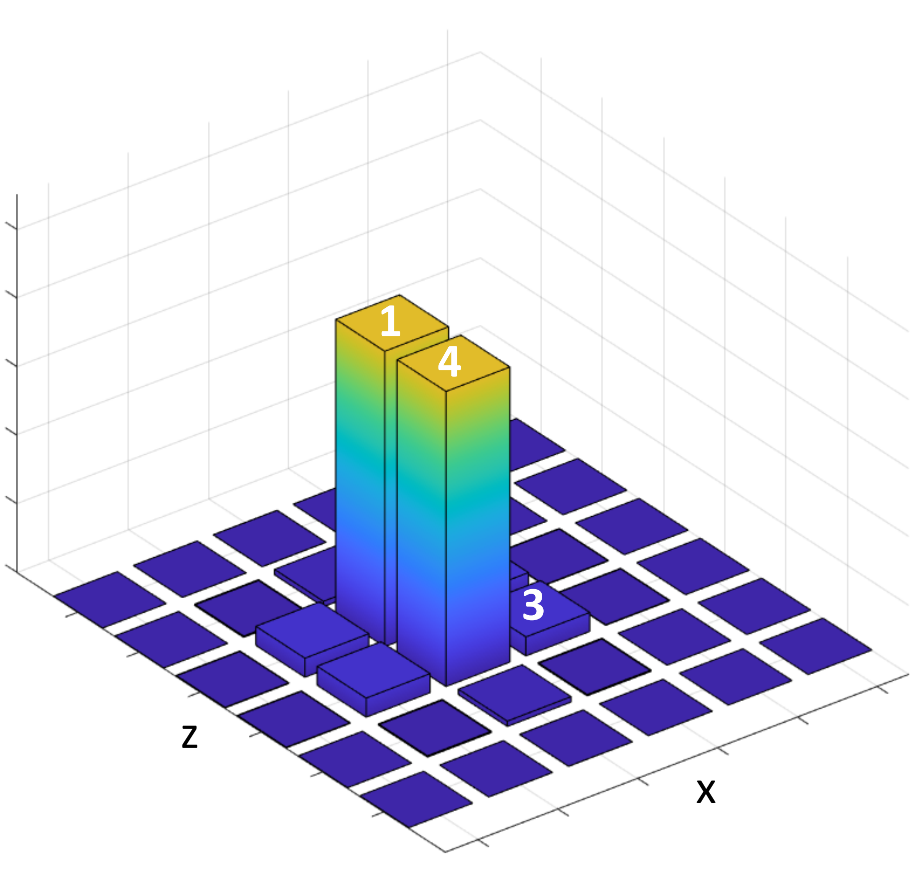

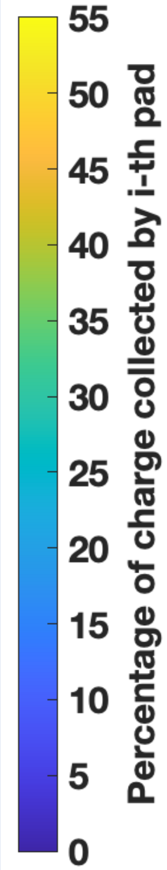

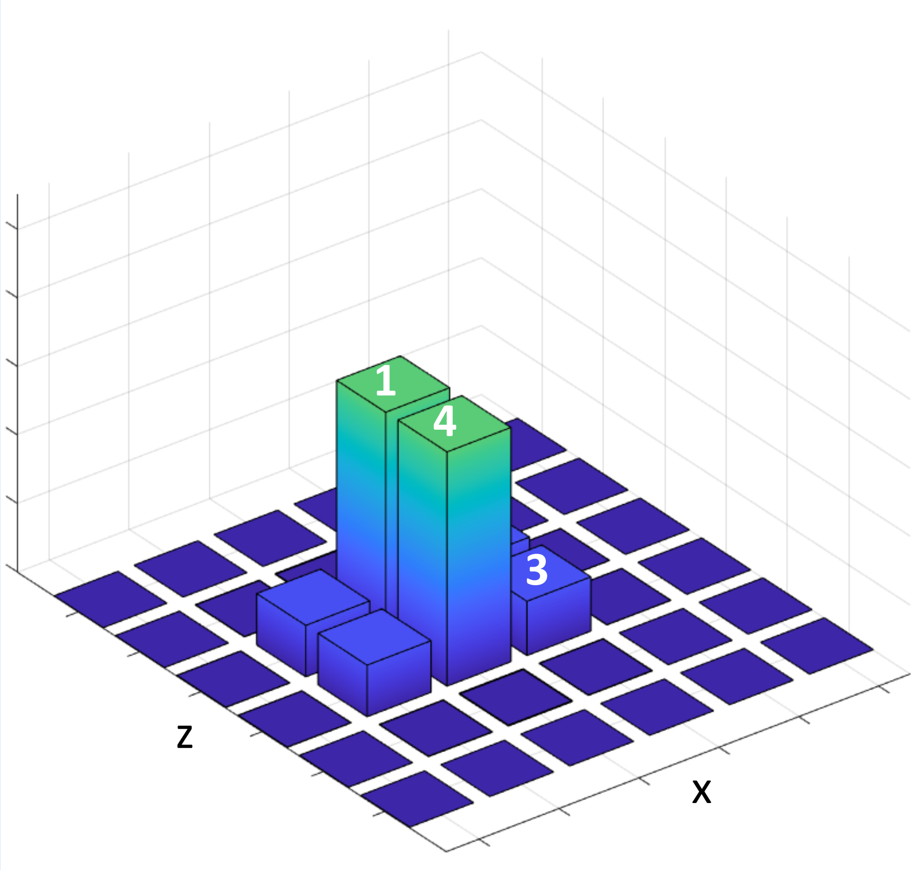

Different pad arrangements

Matrices of squares

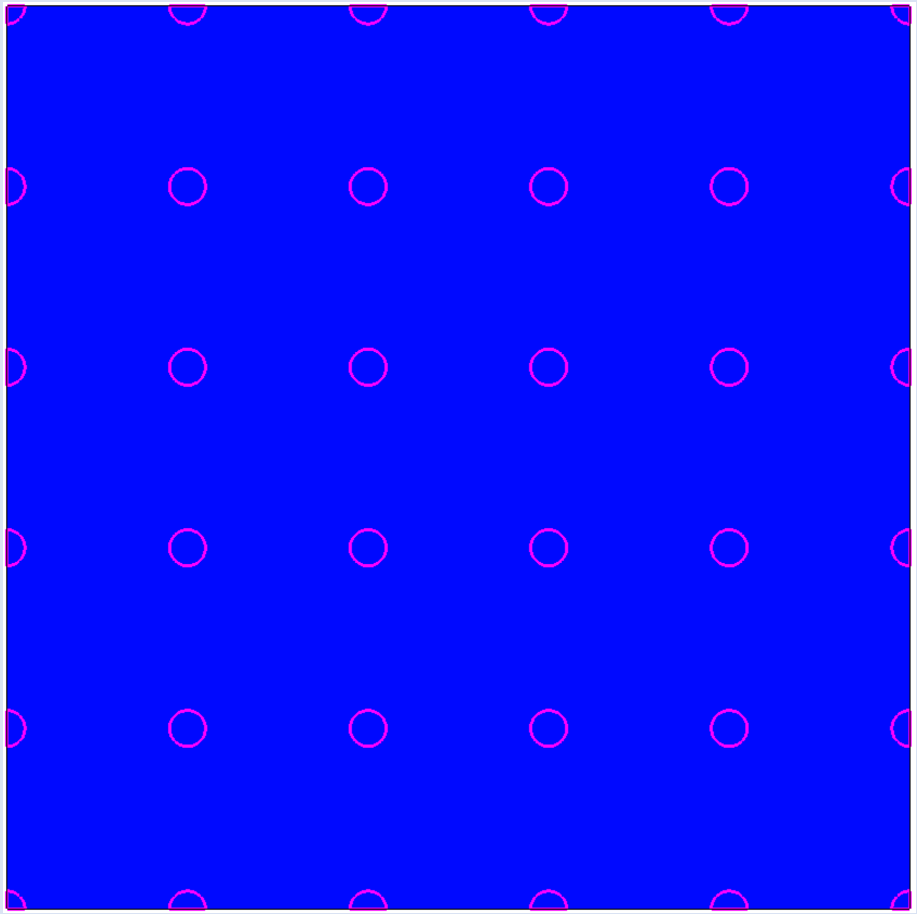

Matrices of triangles